

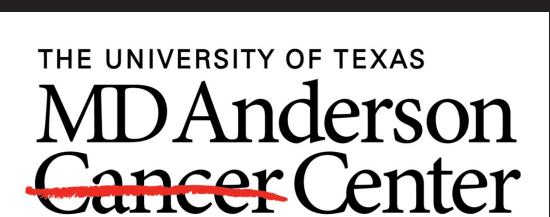


An analytical reconstruction method for integrated mode proton radiography using 2D lateral projections

Mikaël Simard¹, Daniel G. Robertson², Ryan Fullarton¹, Sam Beddar³, Charles-Antoine Collins Fekete¹

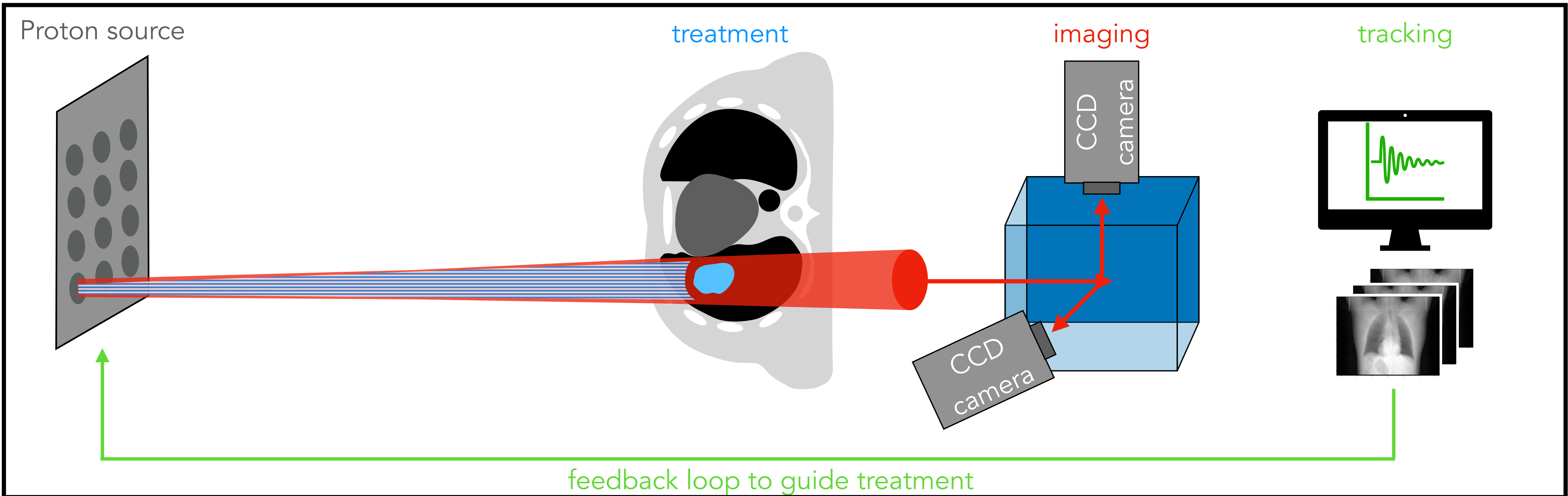


(1) Medical Physics & Biomedical Engineering - University College London. (2) Medical Physics, Department of Radiation Oncology, Mayo Clinic Arizona. (3) Department of Radiation Physics, University of Texas MD Anderson Cancer Center



Introduction - a proton imaging device for tracking

- **Rationale:** design a easily integrable, fast, low cost, **integrated mode proton radiography system** to provide image guidance for cancers that may benefit from escalated dose with proton therapy (e.g. non-small cell lung cancer [1,2])



- **Other potential avenues:**

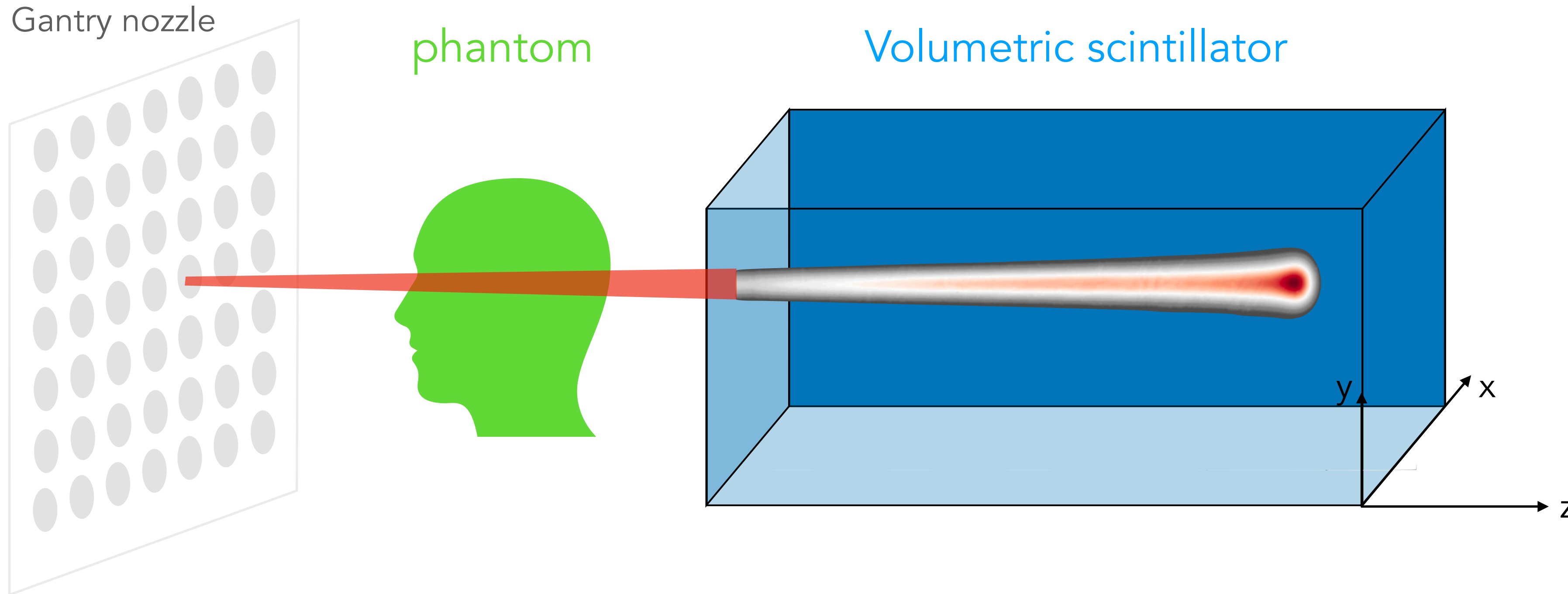
- Potentially low dose solution for positioning
- Use as a QA device to evaluate treatment plans and range measurements (see **R Fullarton's** talk Friday)

[1] Landau et al, Int J Radiation Oncol Biol Phys 95.5 2016.

[2] Bradley et al, Lancet Oncol 16 2015.

Introduction - proposed imaging device

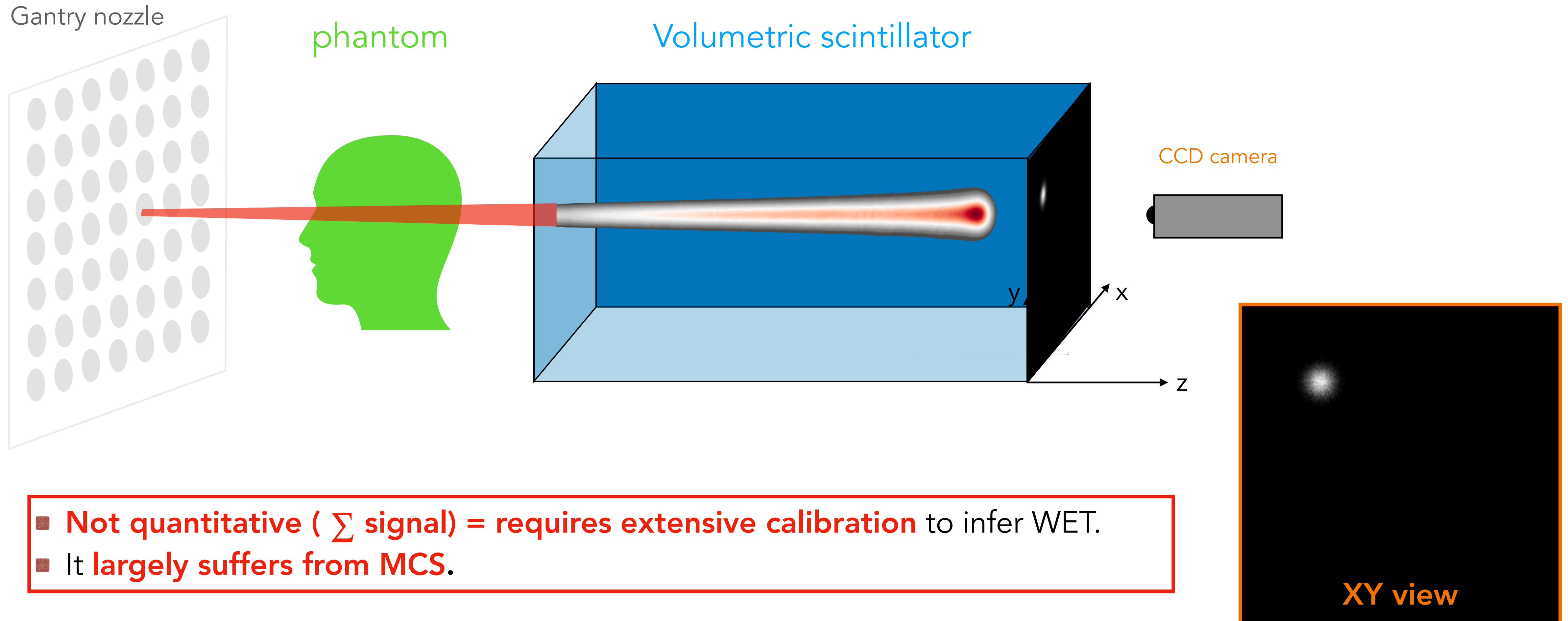
- Consider a **pencil beam scanning** system with a **volumetric scintillator**:



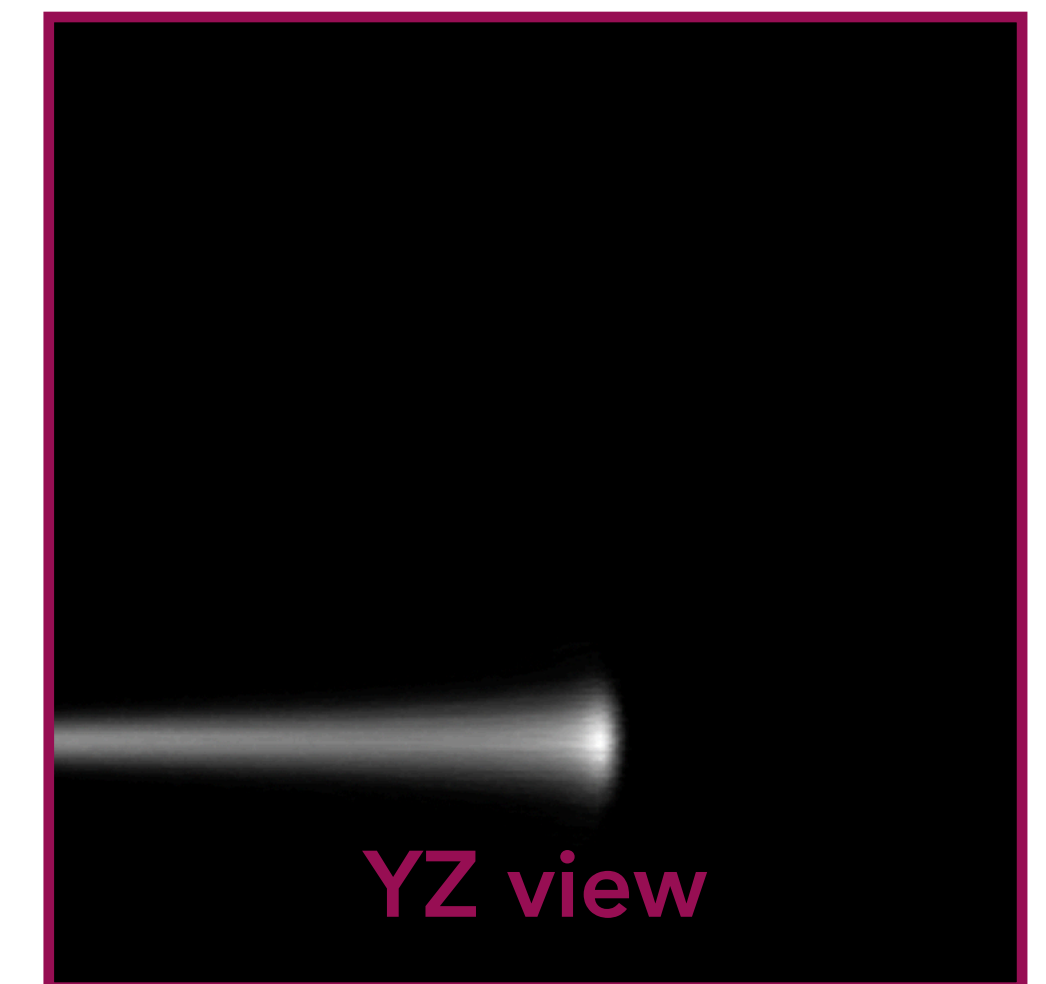
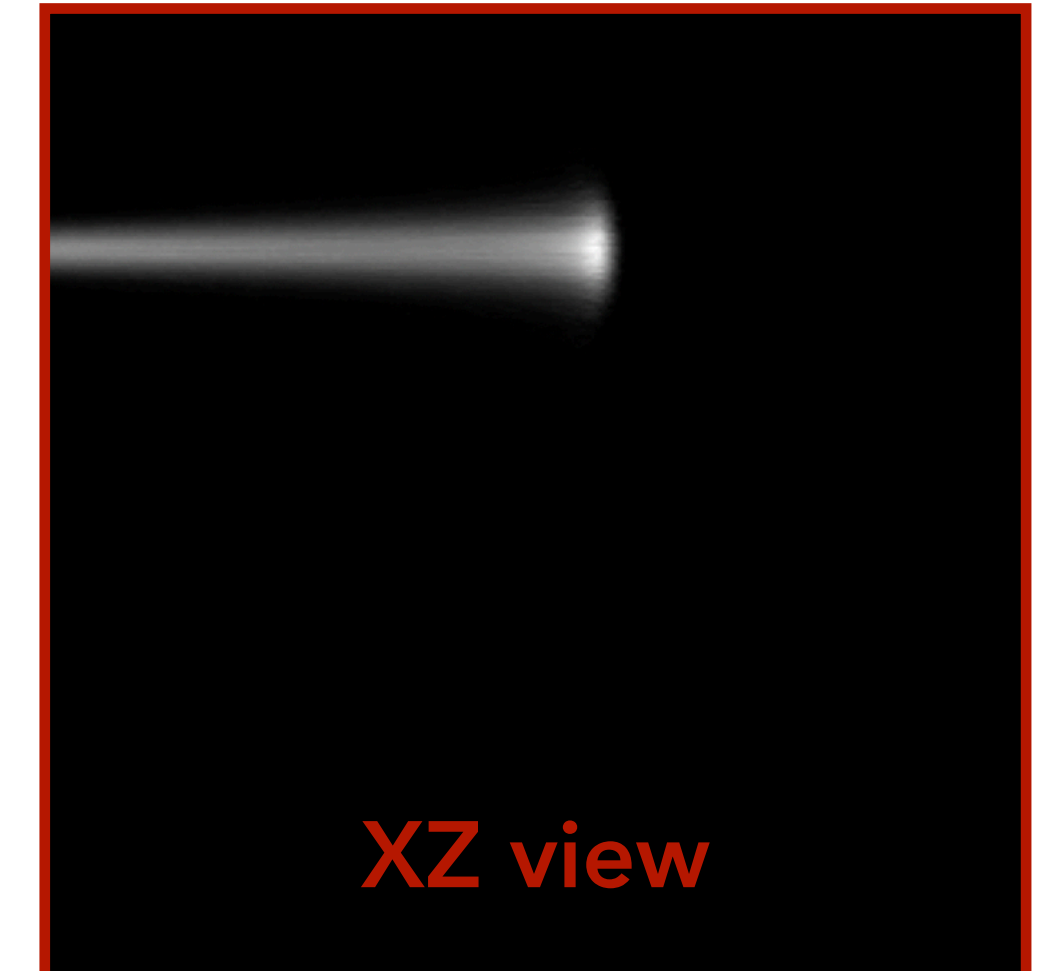
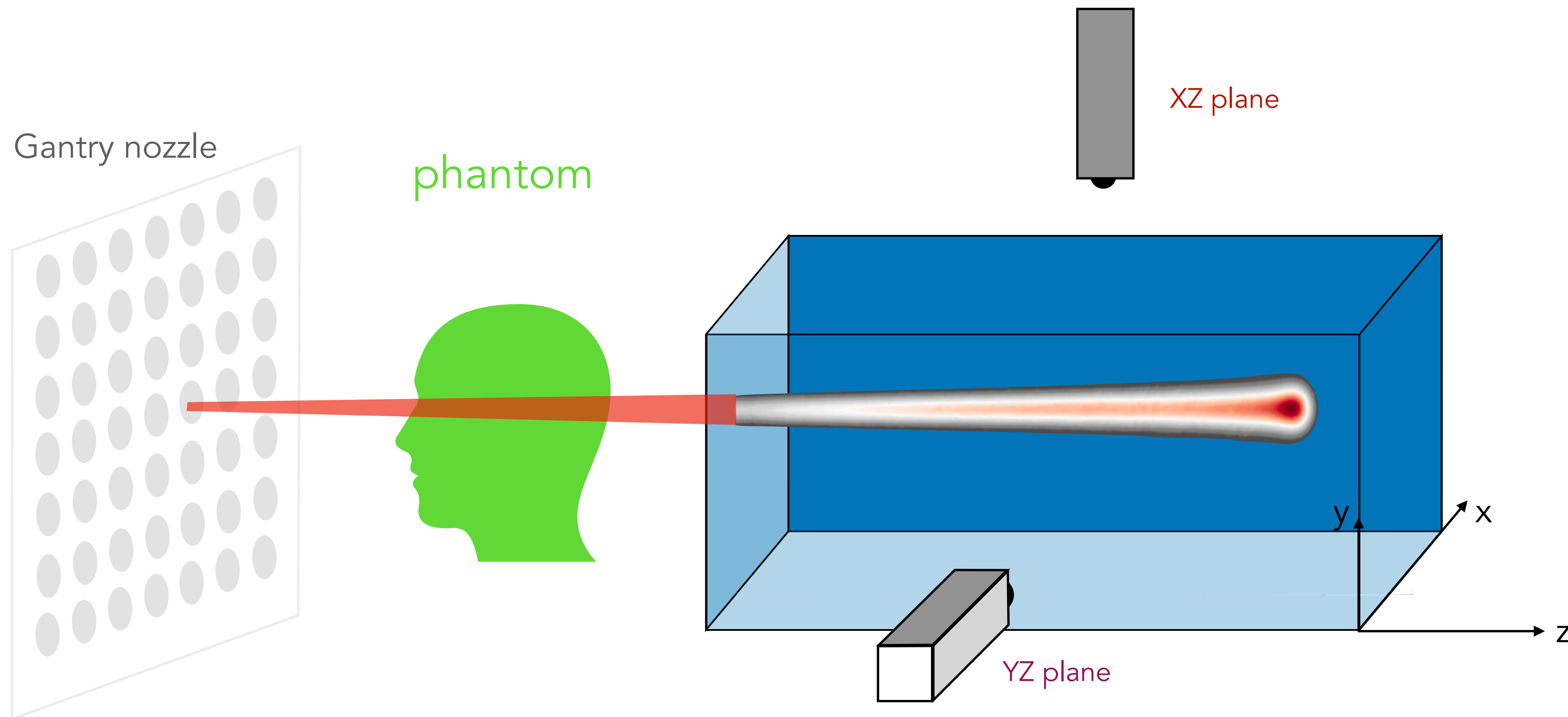
- This setup acquires a **3D quenched light emission distribution** \approx a **3D dose distribution** of **one pencil beam** within the scintillator. **2D projections** of this 3D distribution can be captured using an optical imaging system (*i.e.* CCD cameras).
- See **R Fullarton's** talk Friday for technical details.

Introduction - distal views

- This setup captures a **beam eye** view or **distal** view (XY projection) of the **3D quenched light emission**.

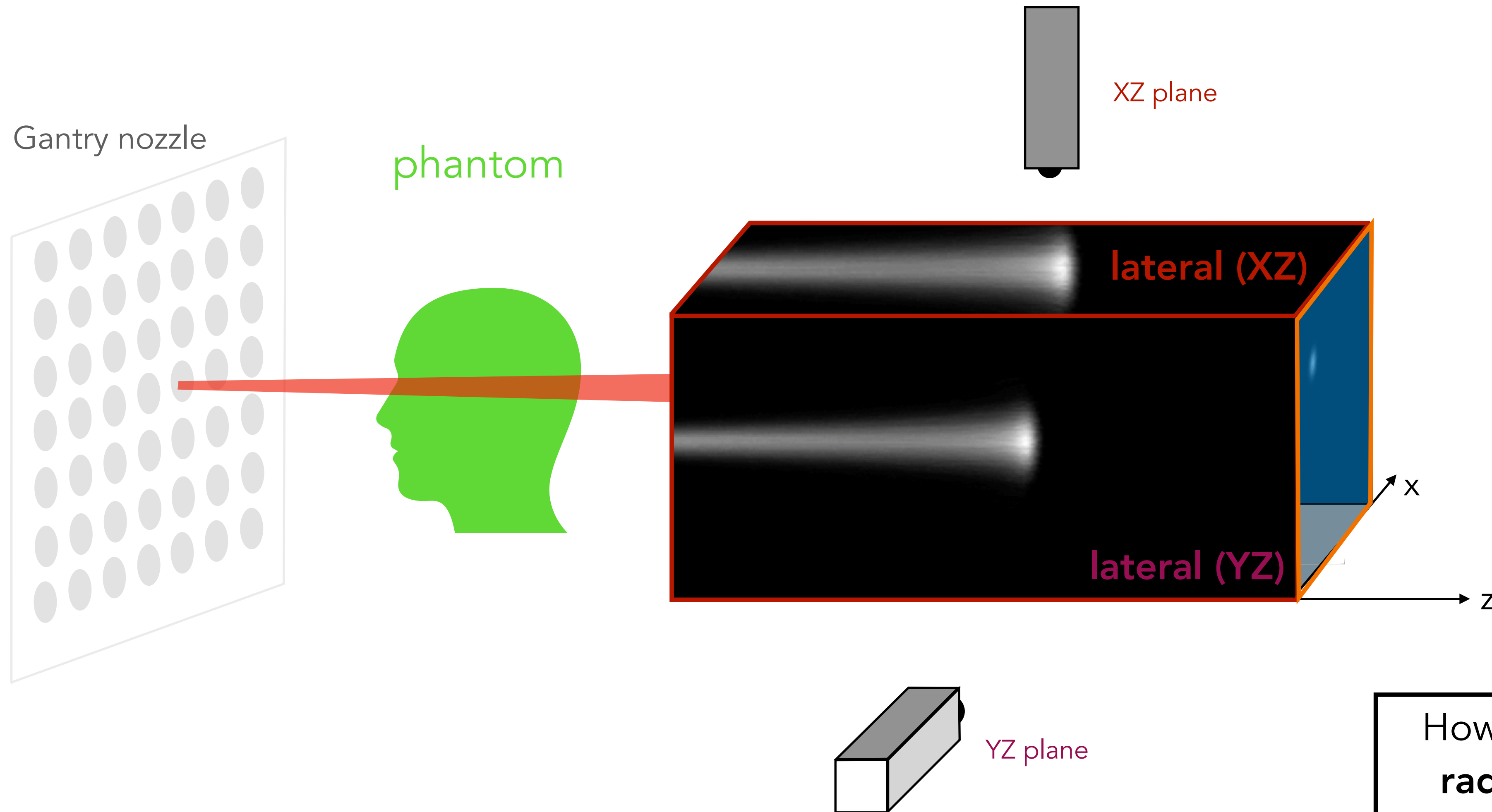


Introduction - lateral views



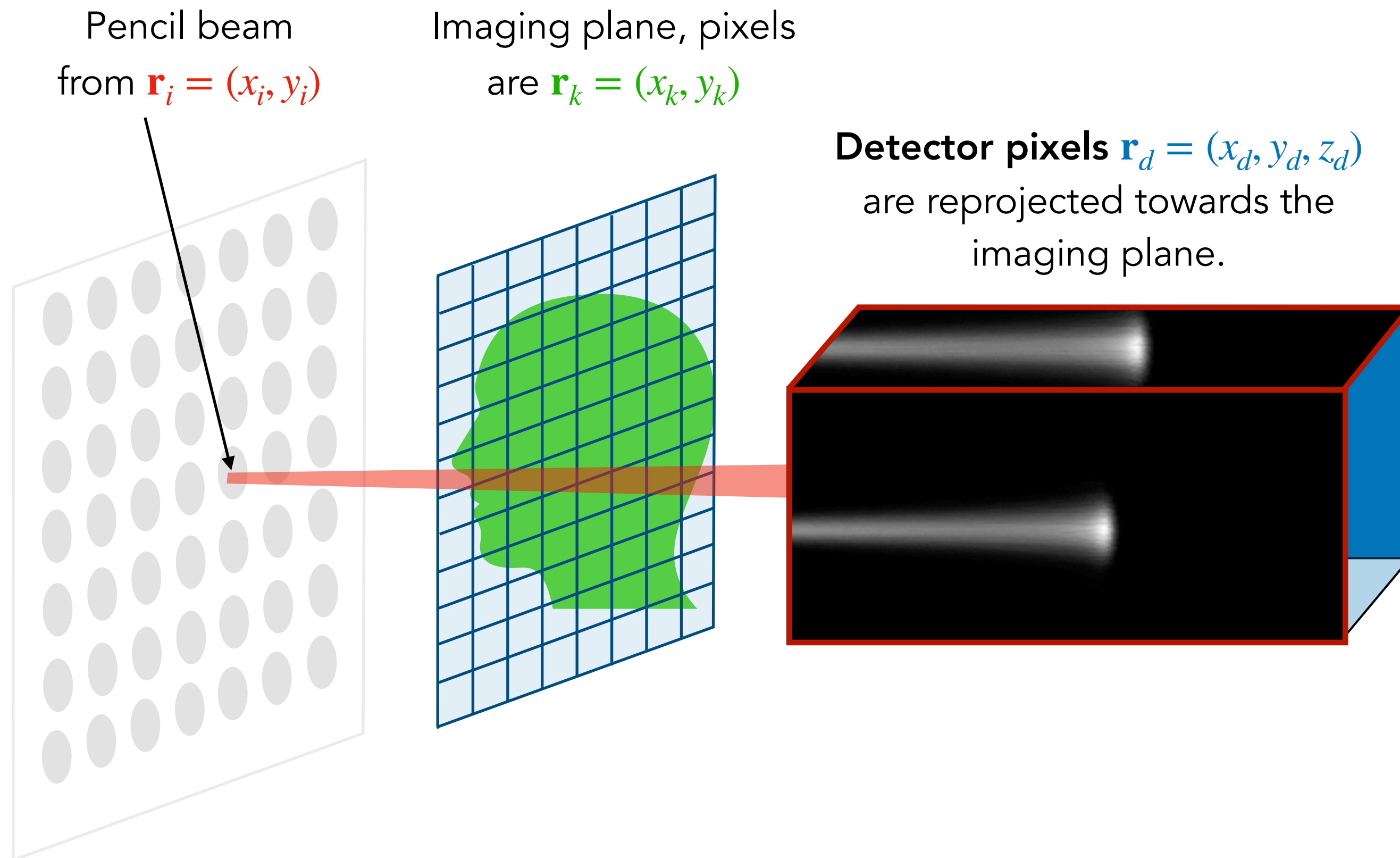
- ✓ Lateral views provide **quantitative information** (WET of traversed material)
- ✓ **Combining both** views can provide **3D positional information** on energy deposition.

Introduction - lateral views

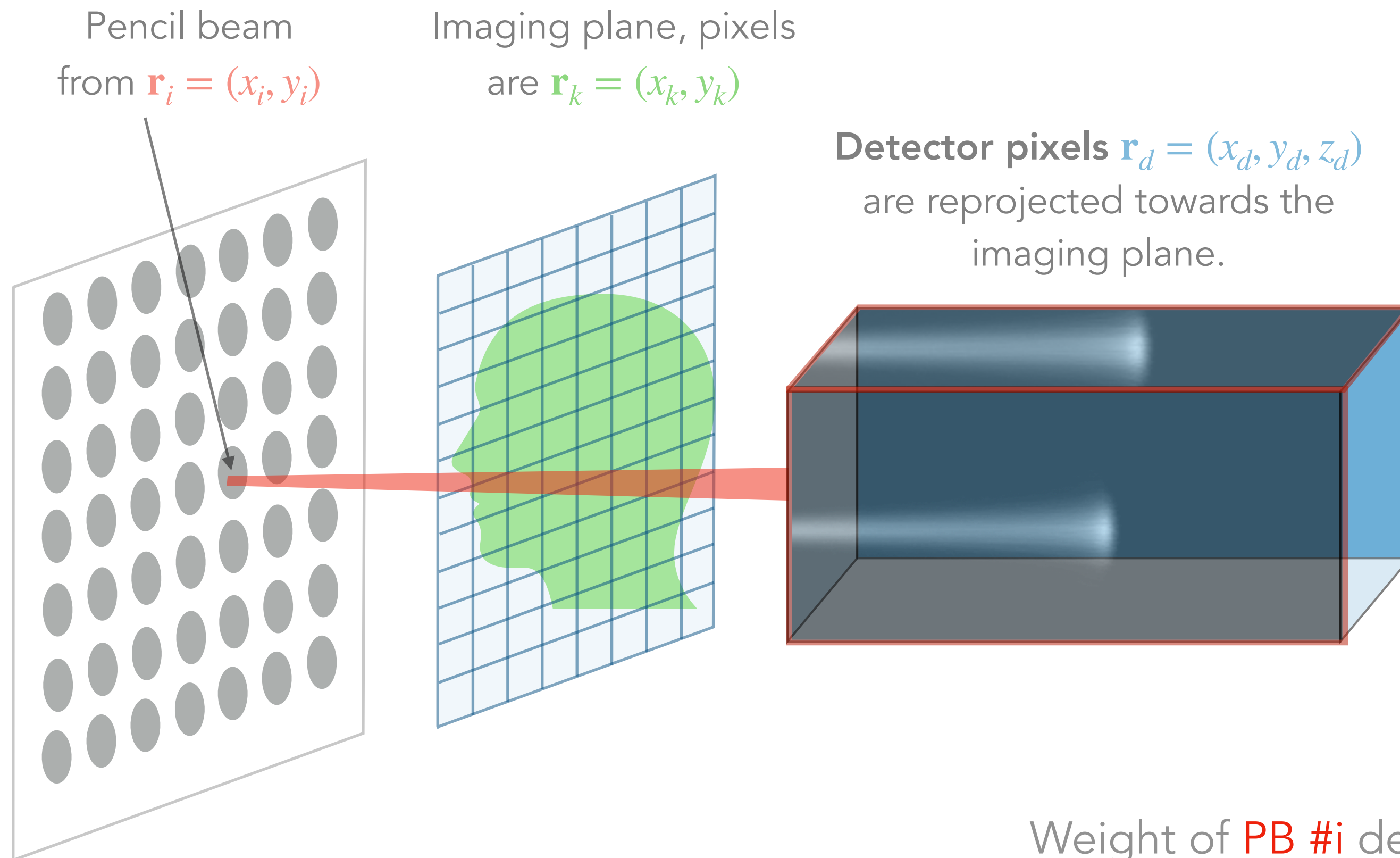


How can we reconstruct **proton radiographs** using the 2 x 2D lateral views?

Reconstruction - 2 x 2D lateral views



Reconstruction - 2 x 2D lateral views



Radiograph

Sum over all PBs

WET of PB #i at depth \mathbf{r}_d

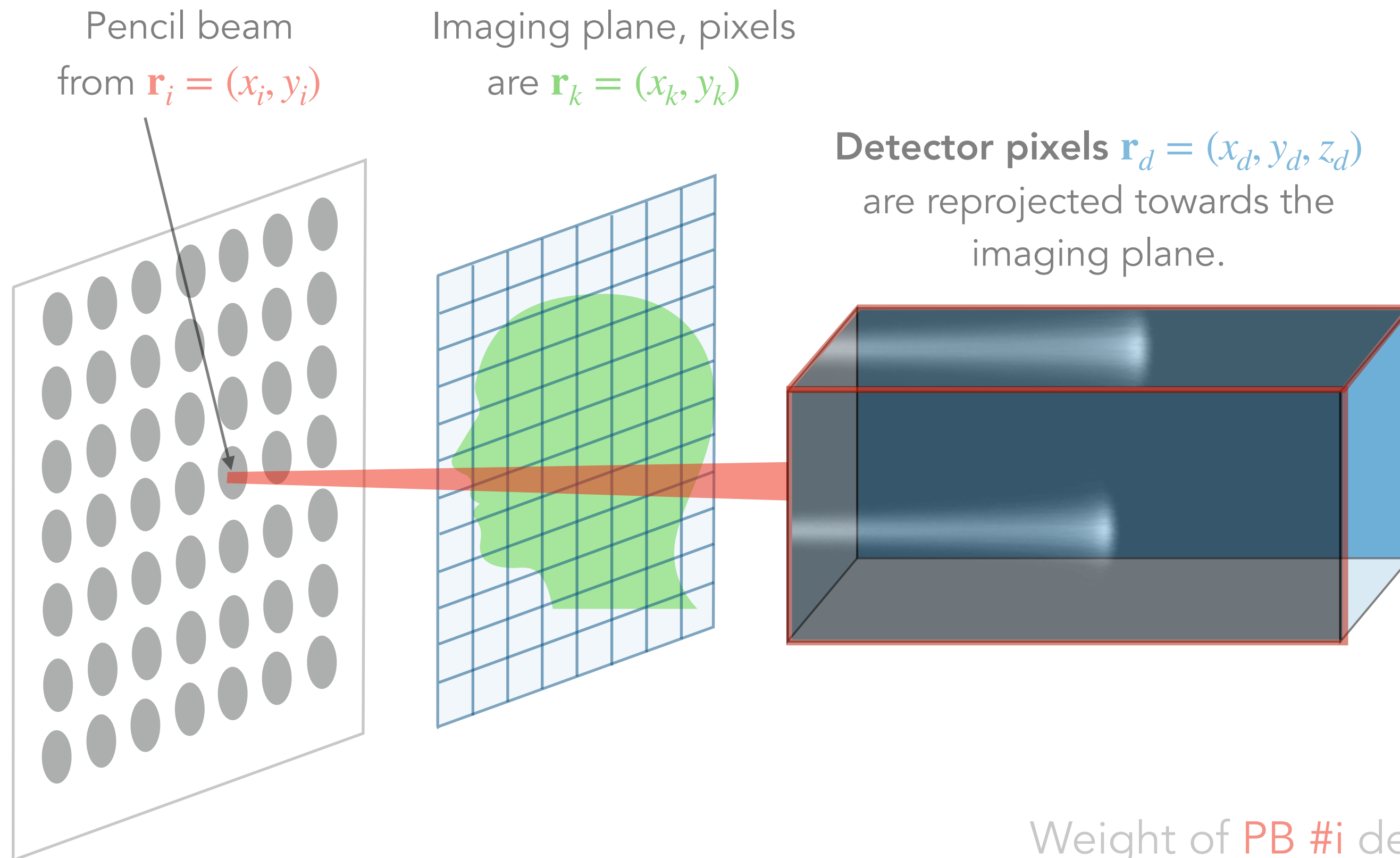
Sum over detector pixels

$$g(\mathbf{r}_k) = \frac{\sum_{i=1}^{n_{PB}} \sum_d w_i(\mathbf{r}_k, \mathbf{r}_d) \frac{N_i(\mathbf{r}_d)}{N_{i,tot}} \text{WET}_i(\mathbf{r}_d)}{\sum_{i=1}^{n_{PB}} \sum_d w_i(\mathbf{r}_k, \mathbf{r}_d) \frac{N_i(\mathbf{r}_d)}{N_{i,tot}}}$$

Weight of PB #i detected at \mathbf{r}_d for imaging pixel \mathbf{r}_k .

Fraction of **protons** that deposit energy at \mathbf{r}_d (filters out low signal)

Reconstruction - 2 x 2D lateral views



Radiograph

Sum over all PBs

Sum over detector pixels

WET of PB #i at depth \mathbf{r}_d

$$g(\mathbf{r}_k) = \frac{\sum_{i=1}^{n_{PB}} \sum_d w_i(\mathbf{r}_k, \mathbf{r}_d) \frac{N_i(\mathbf{r}_d)}{N_{i,tot}} \text{WET}_i(\mathbf{r}_d)}{\sum_{i=1}^{n_{PB}} \sum_d w_i(\mathbf{r}_k, \mathbf{r}_d) \frac{N_i(\mathbf{r}_d)}{N_{i,tot}}}$$

Weight of PB #i detected at \mathbf{r}_d for imaging pixel \mathbf{r}_k .

Fraction of **protons** that deposit energy at \mathbf{r}_d (filters out low signal)

- $w_i(\mathbf{r}_k, \mathbf{r}_d)$: **physics-based** calculation (multiple Coloumb scattering based on Fermi-Eyges theory) that depends on PB and scintillator properties (spot size, angular divergence, emittance, scintillator material) and various geometric assumptions.

Reconstruction - PB weights

- The pencil beam / detector pixel weights $w_i(\mathbf{r}_k, \mathbf{r}_d)$ are the probability of passing through the imaging plane pixel \mathbf{r}_k given that the pencil beam comes from \mathbf{r}_i and is detected at \mathbf{r}_d :

$$w_i(\mathbf{r}_k, \mathbf{r}_d) \equiv P(\mathbf{r}_k | \mathbf{r}_i, \mathbf{r}_d) = \frac{P(\mathbf{r}_k | \mathbf{r}_i)P(\mathbf{r}_d | \mathbf{r}_k, \mathbf{r}_i)}{P(\mathbf{r}_d | \mathbf{r}_i)}$$

Reconstruction - PB weights

- The pencil beam / detector pixel weights $w_i(\mathbf{r}_k, \mathbf{r}_d)$ are the probability of passing through the imaging plane pixel \mathbf{r}_k given that the pencil beam comes from \mathbf{r}_i and is detected at \mathbf{r}_d :

$$w_i(\mathbf{r}_k, \mathbf{r}_d) \equiv P(\mathbf{r}_k | \mathbf{r}_i, \mathbf{r}_d) = \frac{P(\mathbf{r}_k | \mathbf{r}_i)P(\mathbf{r}_d | \mathbf{r}_k, \mathbf{r}_i)}{P(\mathbf{r}_d | \mathbf{r}_i)}$$

Reconstruction - PB weights

- The pencil beam / detector pixel weights $w_i(\mathbf{r}_k, \mathbf{r}_d)$ are the probability of passing through the imaging plane pixel \mathbf{r}_k given that the pencil beam comes from \mathbf{r}_i and is detected at \mathbf{r}_d :

$$w_i(\mathbf{r}_k, \mathbf{r}_d) \equiv P(\mathbf{r}_k | \mathbf{r}_i, \mathbf{r}_d) = \frac{P(\mathbf{r}_k | \mathbf{r}_i)P(\mathbf{r}_d | \mathbf{r}_k, \mathbf{r}_i)}{P(\mathbf{r}_d | \mathbf{r}_i)}$$

- The probability $P(\mathbf{r}_k | \mathbf{r}_i)$ is known [3] for a Gaussian beam with the following location PDF: $p(\mathbf{r} | \mathbf{r}_i) = \frac{1}{\pi\sigma_l^2(z)} \exp\left(-\frac{(x-x_i)^2 + (y-y_i)^2}{\sigma_l^2(z)}\right)$
- $P(\mathbf{r}_k | \mathbf{r}_i)$ is the marginalised beam location PDF over each reconstruction pixel:

$$P(\mathbf{r}_k | \mathbf{r}_i) = \int_{z_k-\delta_k}^{z_k+\delta_k} \int_{y_k-\delta_k}^{y_k+\delta_k} \int_{x_k-\delta_k}^{x_k+\delta_k} p(\mathbf{r} | \mathbf{r}_i) dx dy dz = \frac{1}{4} \left(\operatorname{erf}\left(\frac{x_k - x_i + \delta_k}{\sigma_l(z_k)}\right) - \operatorname{erf}\left(\frac{x_k - x_i - \delta_k}{\sigma_l(z_k)}\right) \right) \left(\operatorname{erf}\left(\frac{y_k - y_i + \delta_k}{\sigma_l(z_k)}\right) - \operatorname{erf}\left(\frac{y_k - y_i - \delta_k}{\sigma_l(z_k)}\right) \right)$$

- The spatial spread of the beam $\sigma_l^2(z)$ depends on **geometric spread** and **multiple Coulomb scattering**:

$$\sigma_l^2(z_0, z) = \underbrace{\sigma_l^2(z_0) + 2\sigma_{l\theta_l}(z_0)z + \sigma_{\theta_l}^2(z_0)z^2}_{\text{geometric spread}} + \underbrace{\mathcal{A}_2(z_0, z)}_{\text{multiple Coulomb scattering}} \quad \mathcal{A}_n(z_0, z) = Z^2 E_0^2 \left(1 + 0.038 \ln \left(\int_{z_0}^z \frac{dz'}{X_0(z')} \right) \right)^2 \int_{z_0}^z \frac{(z-z')^n}{p^2(z')\beta^2(z')X_0(z')} dz'$$

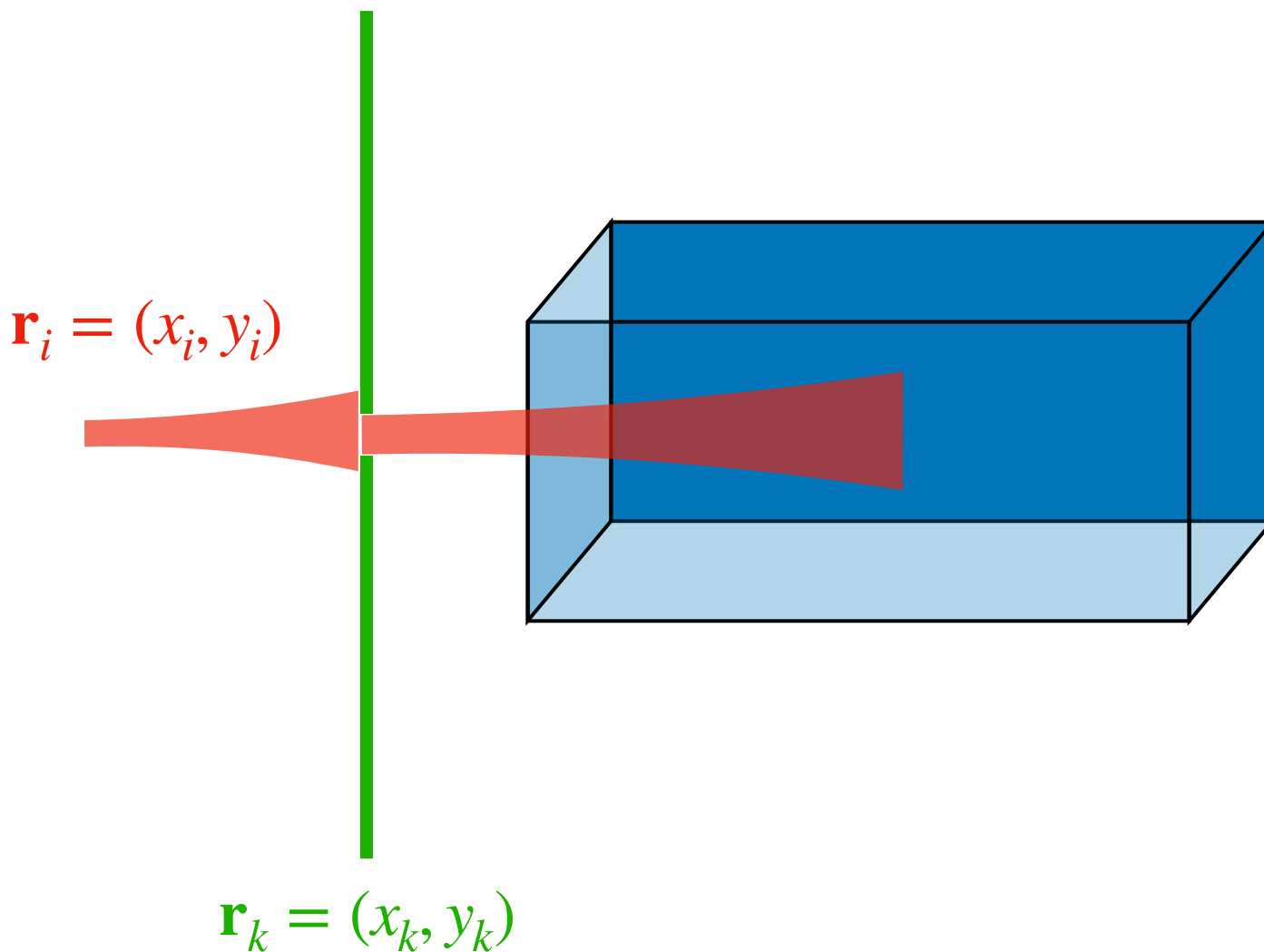
- $P(\mathbf{r}_d | \mathbf{r}_i)$ has the same expression, but the beam spread $\sigma_l^2(z)$ includes extra scattering/divergence through the object and detector.

Reconstruction - PB weights

- The pencil beam / detector pixel weights $w_i(\mathbf{r}_k, \mathbf{r}_d)$ are the probability of passing through the imaging plane pixel \mathbf{r}_k given that the pencil beam comes from \mathbf{r}_i and is detected at \mathbf{r}_d :

$$w_i(\mathbf{r}_k, \mathbf{r}_d) \equiv P(\mathbf{r}_k | \mathbf{r}_i, \mathbf{r}_d) = \frac{P(\mathbf{r}_k | \mathbf{r}_i) P(\mathbf{r}_d | \mathbf{r}_k, \mathbf{r}_i)}{P(\mathbf{r}_d | \mathbf{r}_i)}$$

- The probability $P(\mathbf{r}_d | \mathbf{r}_k, \mathbf{r}_i)$ is calculated using the Fermi-Eyges pencil beam summation method, assuming that the pixel at \mathbf{r}_k acts as a square collimator [4,5]. Solution for the XZ view:



$$P(\mathbf{r}_d | \mathbf{r}_k, \mathbf{r}_i) = \int_{x_d - \delta_d}^{x_d + \delta_d} \frac{1}{N_x \sqrt{\pi \kappa}} \exp\left(-\frac{(x - x_i)^2}{\kappa}\right) \left[\operatorname{erf}\left(\frac{\kappa_2(x - x_k + \delta_k) + \kappa_1(x_i - x_k + \delta_k)}{\sqrt{\Delta \kappa}}\right) - \operatorname{erf}\left(\frac{\kappa_2(x - x_k - \delta_k) + \kappa_1(x_i - x_k + \delta_k)}{\sqrt{\Delta \kappa}}\right) \right]$$

with:

$$\kappa_1 = \mathcal{A}_2(z_d) + \sigma_{x\theta_x}(z_k)(z_d - z_k) + \sigma_{\theta_x}^2(z_k)(z_d - z_k)^2$$

$$\kappa_2 = \sigma_x^2(z_k) + \sigma_{x\theta_x}(z_k)(z_d - z_k)$$

$$\kappa = \kappa_1 + \kappa_2$$

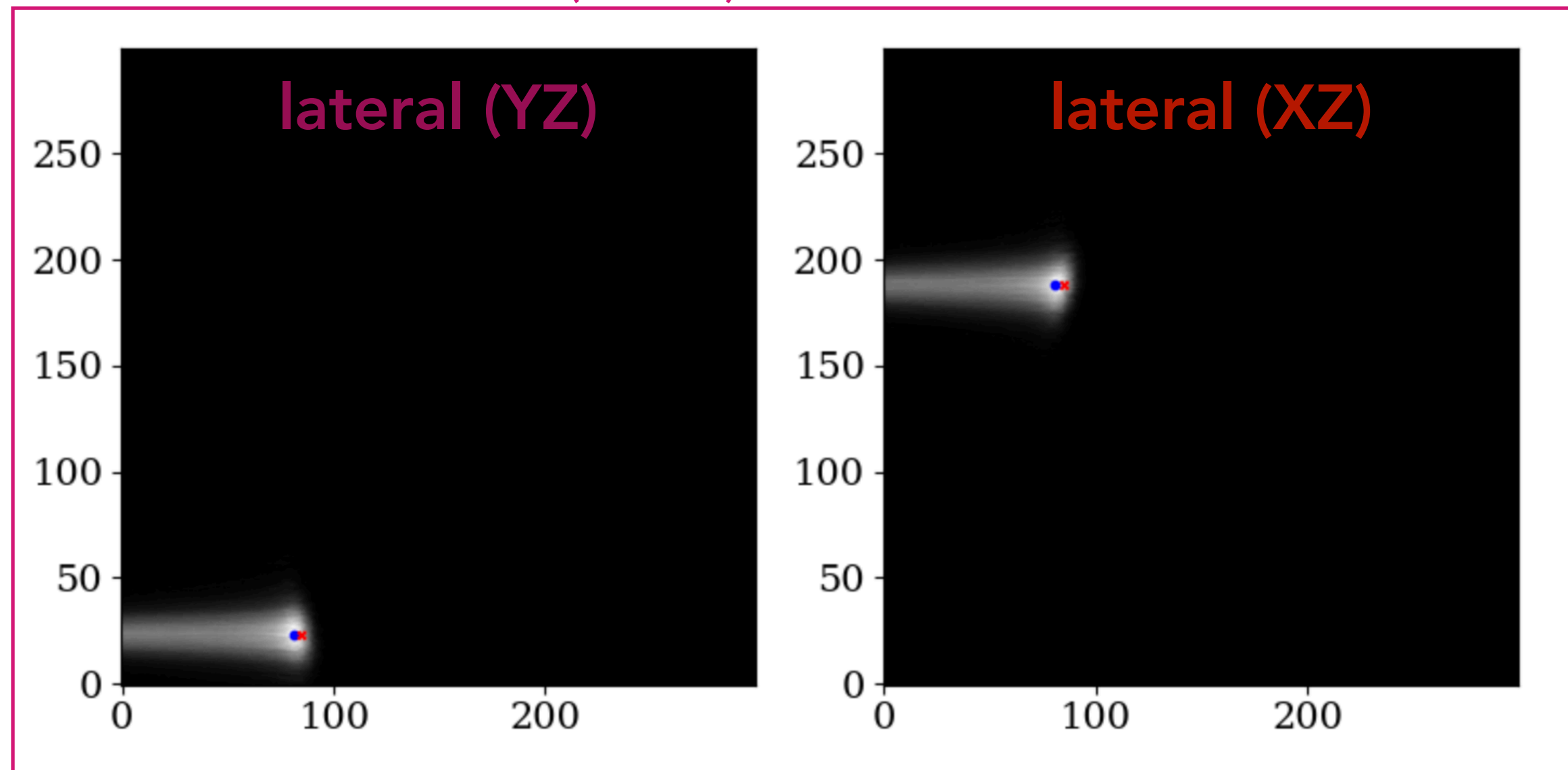
$$\Delta = \sigma_x^2(z_k)\kappa_1 - \sigma_{x\theta_x}(z_k)(z_d - z_k)\kappa_2$$

Reconstruction - an issue with scintillation detectors

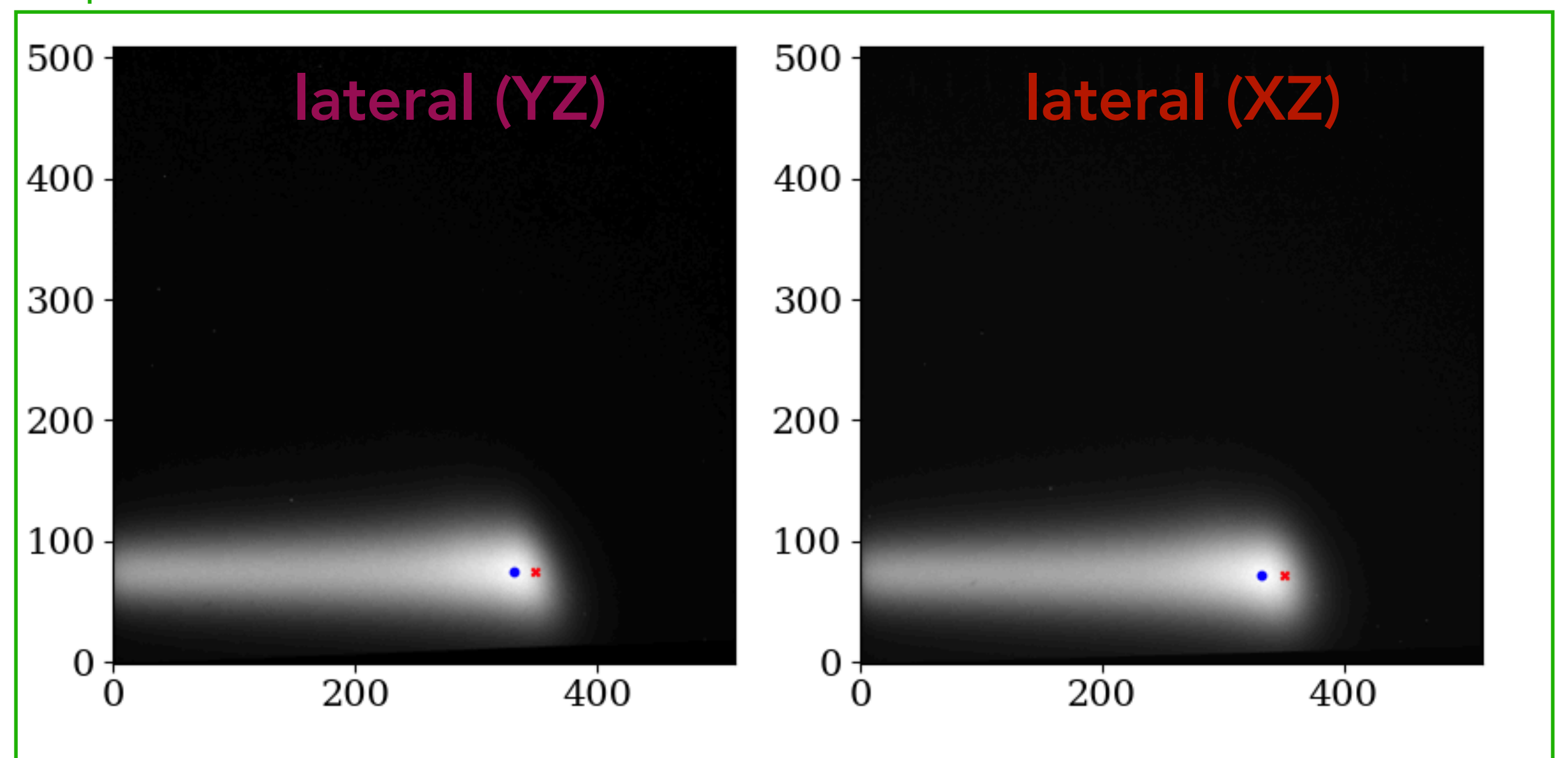
$$g(\mathbf{r}_k) = \frac{\sum_{i=1}^{n_{PB}} w_i(\mathbf{r}_k, \mathbf{r}_d) \frac{N_i(\mathbf{r}_d)}{N_{i,\text{tot}}} \text{WET}_i(\mathbf{r}_d)}{\sum_{i=1}^{n_{PB}} w_i(\mathbf{r}_k, \mathbf{r}_d) \frac{N_i(\mathbf{r}_d)}{N_{i,\text{tot}}}}$$

- The **fraction of particles depositing energy** is not directly measurable or easy to extract using **scintillation data**.
- **For now**, we consider the alternative of selecting a subset of useful detector pixels in images, and only back-projecting them -> *peakfinder*.

Monte Carlo dataset (XCAT)



Experimental dataset (Paediatric head)

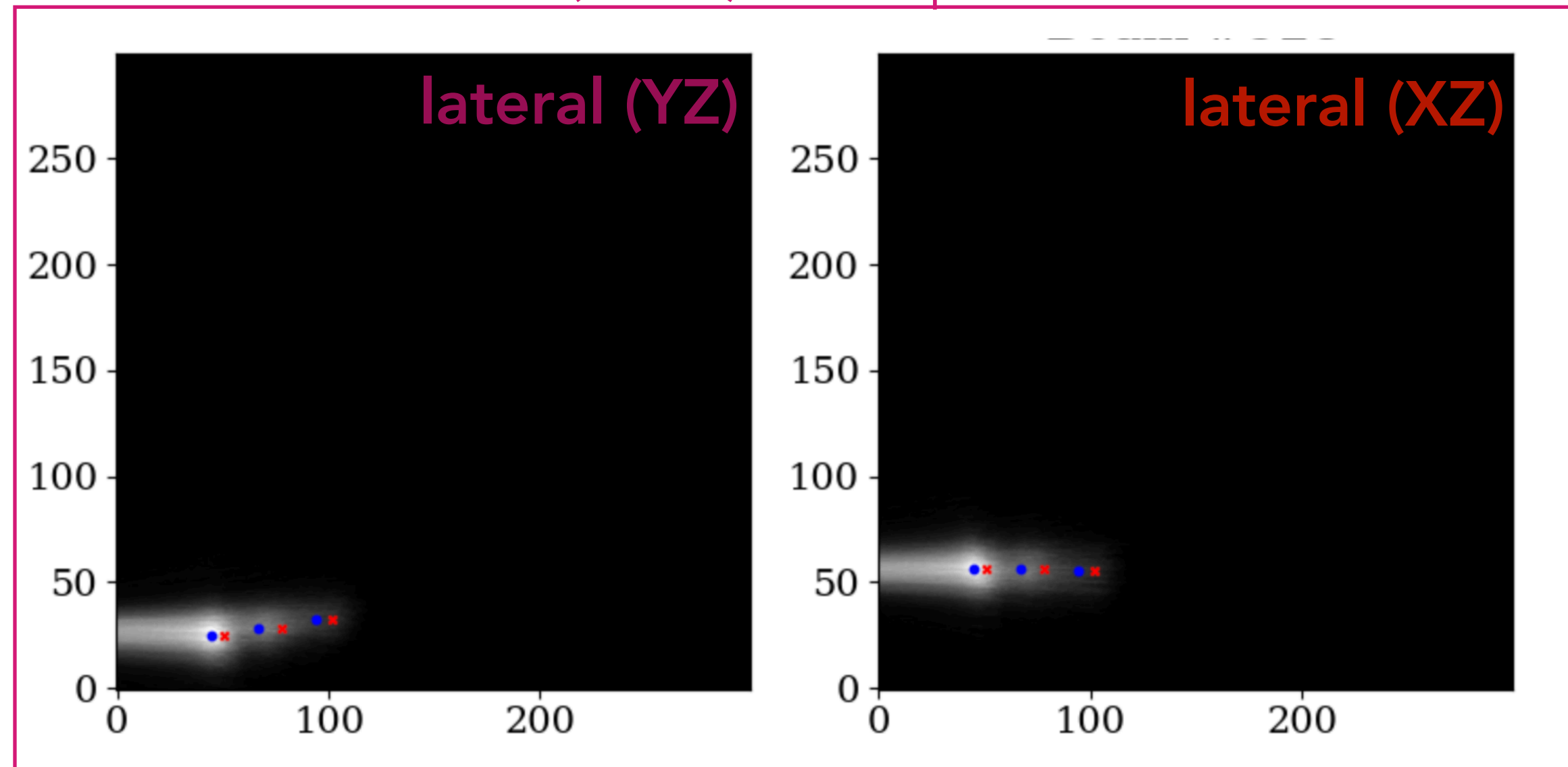


- **Peaks** in the image are found in both lateral views (●) and the probable position of the corresponding range pixel (x) is reprojected.

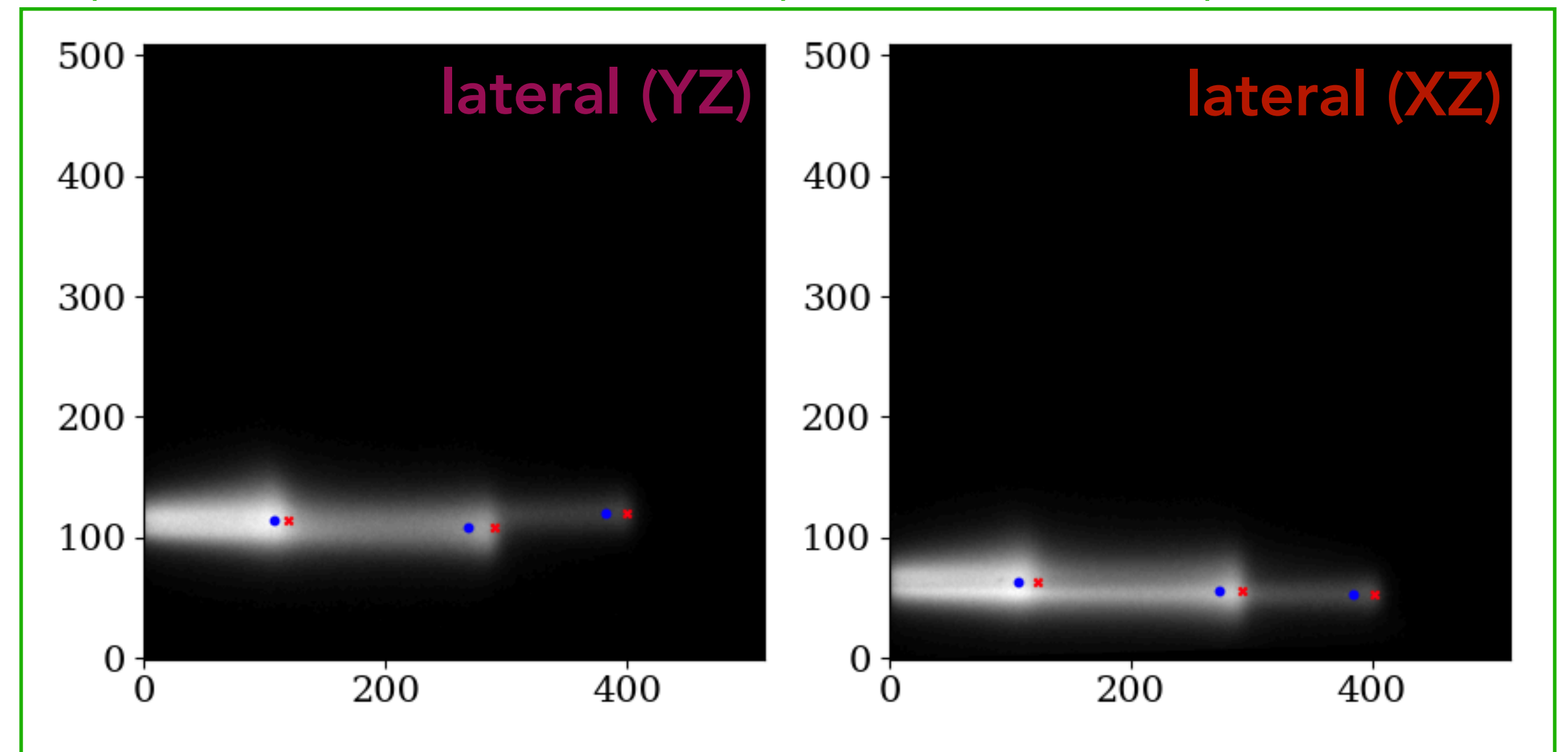
Reconstruction - an issue with scintillation detectors

- The peakfinder can find **multiple peaks** for PBs crossing complex geometries with multiple interfaces

Monte Carlo dataset (XCAT) with 3 peaks



Experimental dataset (MVQA phantom) with 3 peaks



Methods - general

Framework

Monte Carlo data

Experimental data (Mayo Clinic Az)

Phantoms

- **Resolution:** Slanted edge
- **Image quality & WET accuracy:** XCAT

- **Resolution:** Slanted edge, MVQA
- **Contrast:** Las Vegas
- **WET accuracy:** 9 Gammex plugs
- **Image quality:** Paediatric head & thorax

this work

Recon
methods

- 2x2D lateral views
- 2D distal view [6]
- 1D lateral view** [3]
- Single event imaging (ideal trackers)

- 2x2D lateral views
- 1D lateral view** [3]

Methods - general

Framework

Monte Carlo data

Experimental data (Mayo Clinic Az)

Phantoms

- **Resolution:** Slanted edge
- **Image quality & WET accuracy:** XCAT

- **Resolution:** Slanted edge, MVQA
- **Contrast:** Las Vegas
- **WET accuracy:** 9 Gammex plugs
- **Image quality:** Paediatric head & thorax

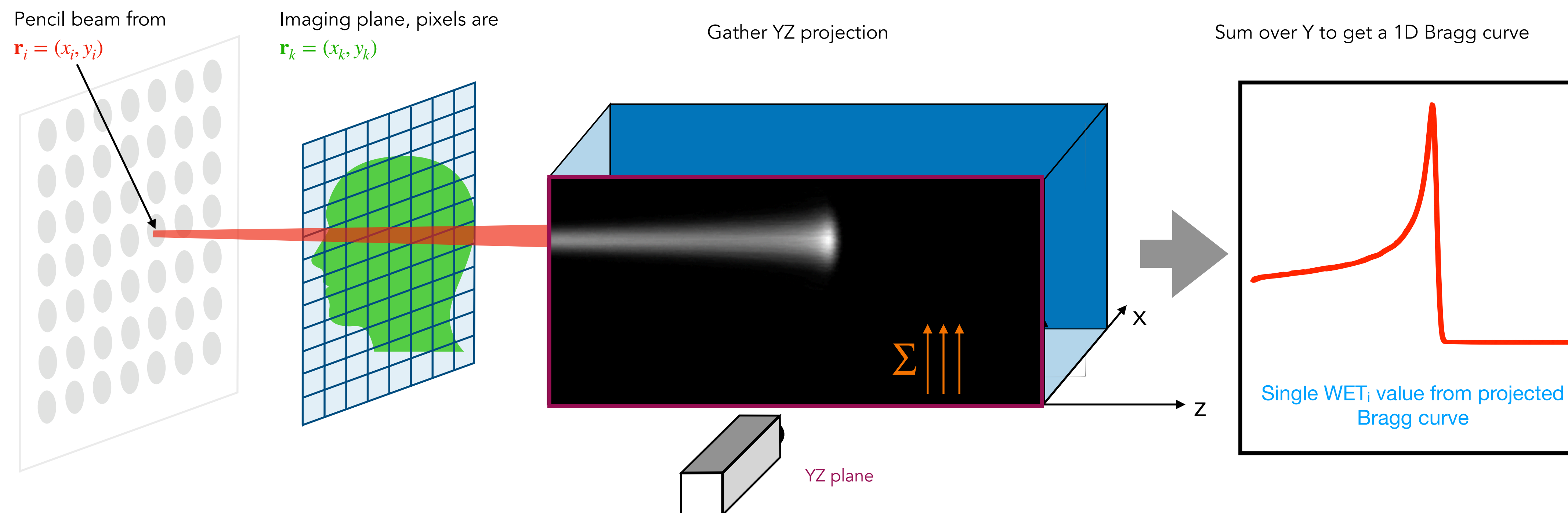
Recon
methods

- 2x2D lateral views
- 2D distal view [6]
- 1D lateral view** [3]
- Single event imaging (ideal trackers)

- 2x2D lateral views
- 1D lateral view** [3]

Methods - comparing 2D vs 1D signals

- Are there **benefits** to using **2D lateral data** (images) against **1D lateral data** (PDD)?
- The algorithm using **2x2D lateral views** is compared to a method using **1D lateral views**.
- The **1D lateral view** is **analogous** to using a **range telescope**. It is simulated as follows:



- The reconstruction method of Rescigno *et al* [3] is used to reproject each WET value to the imaging plane.

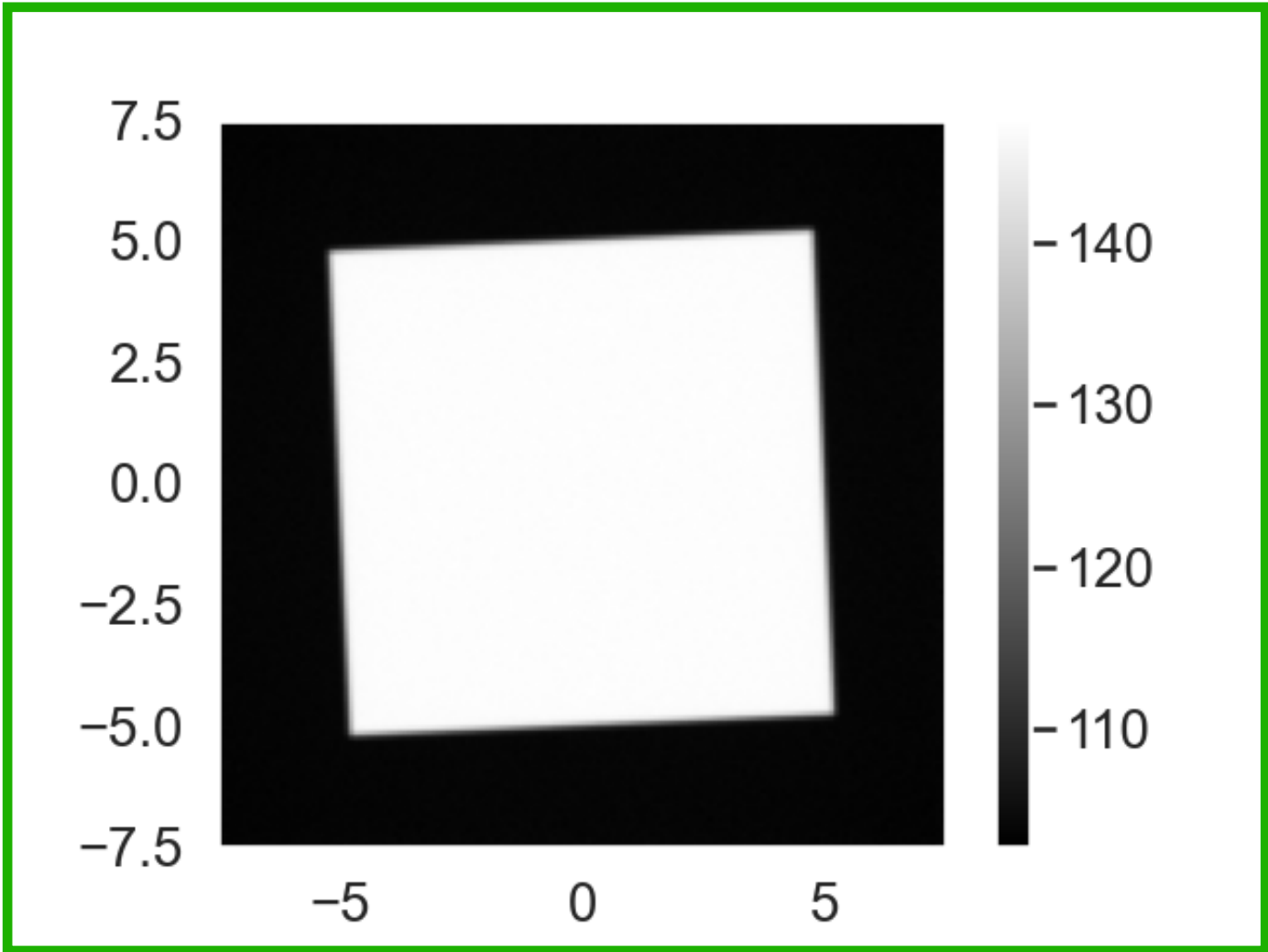
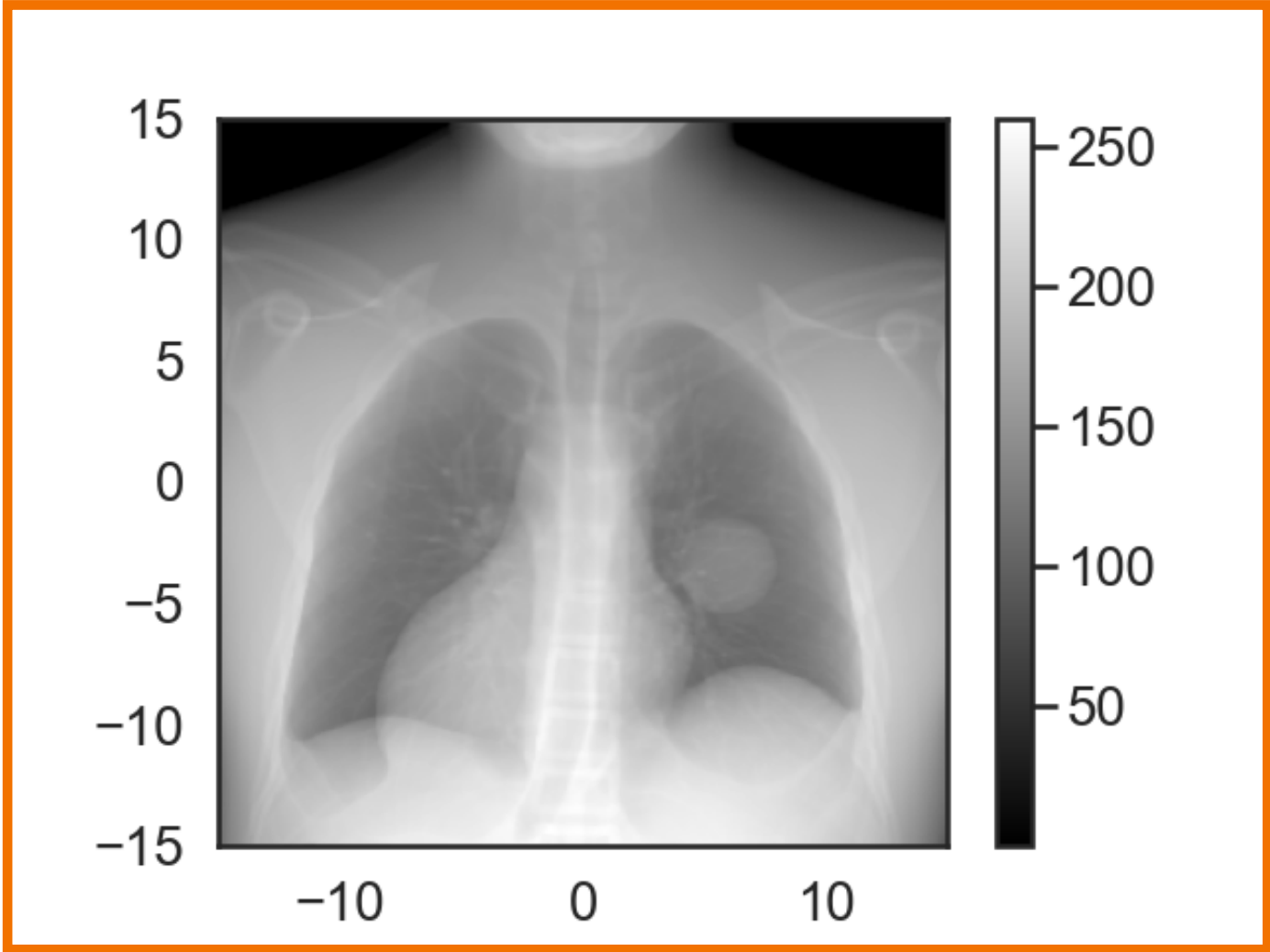
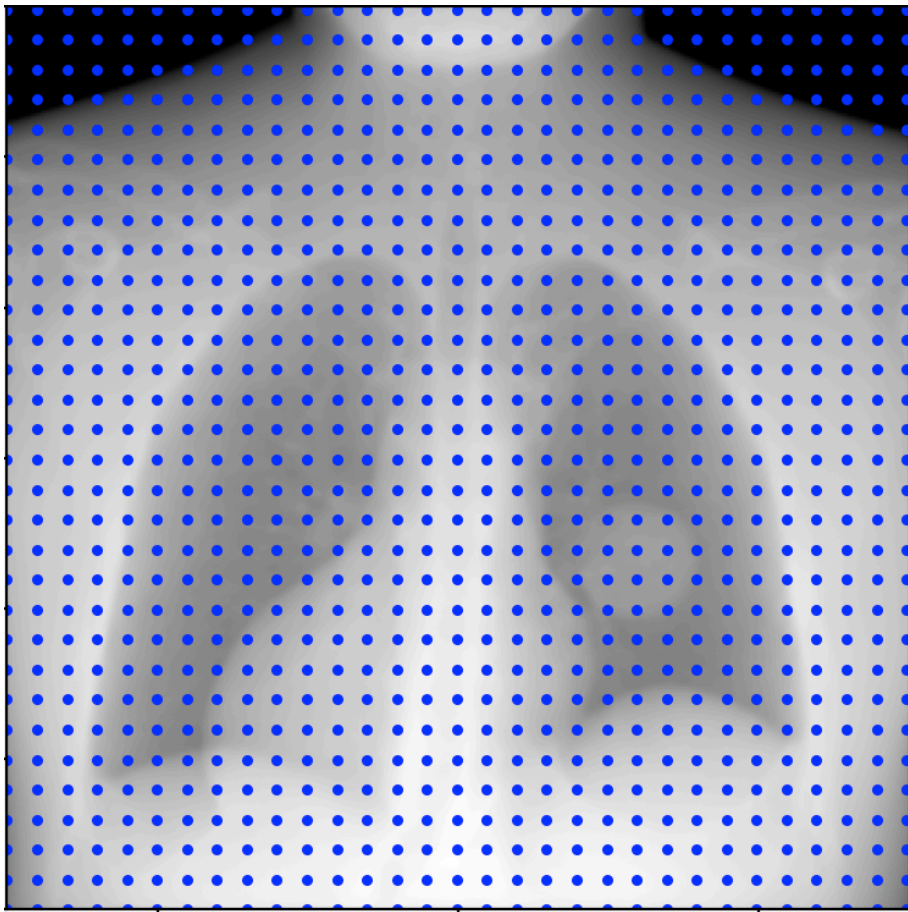
Methods - Geant4 Monte Carlo simulations

- **Quenched light emission** is scored in a 30x30 cm² volumetric scintillator = **non-ideal imaging conditions for integrated mode imaging.**
- **Phantoms:** one phase of extended cardiac thorso **XCAT** (30x30 cm² FOV) and **slanted edge** (15x15 cm² FOV, cube has 5 cm WET inside 10 cm WET water tank)

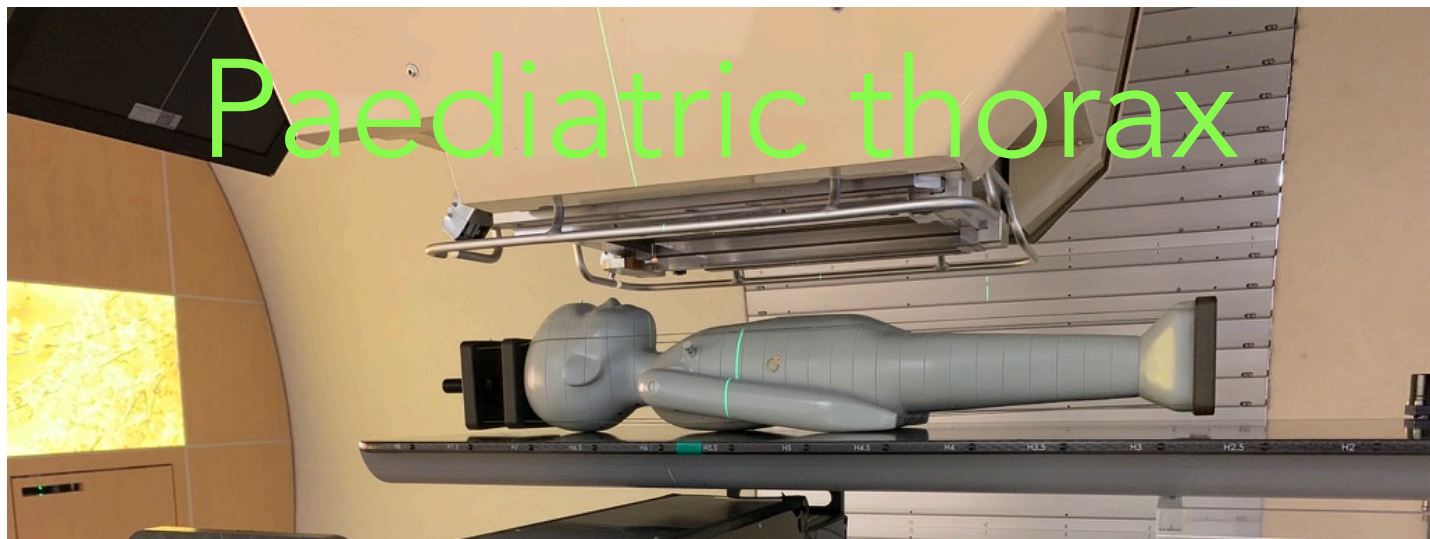
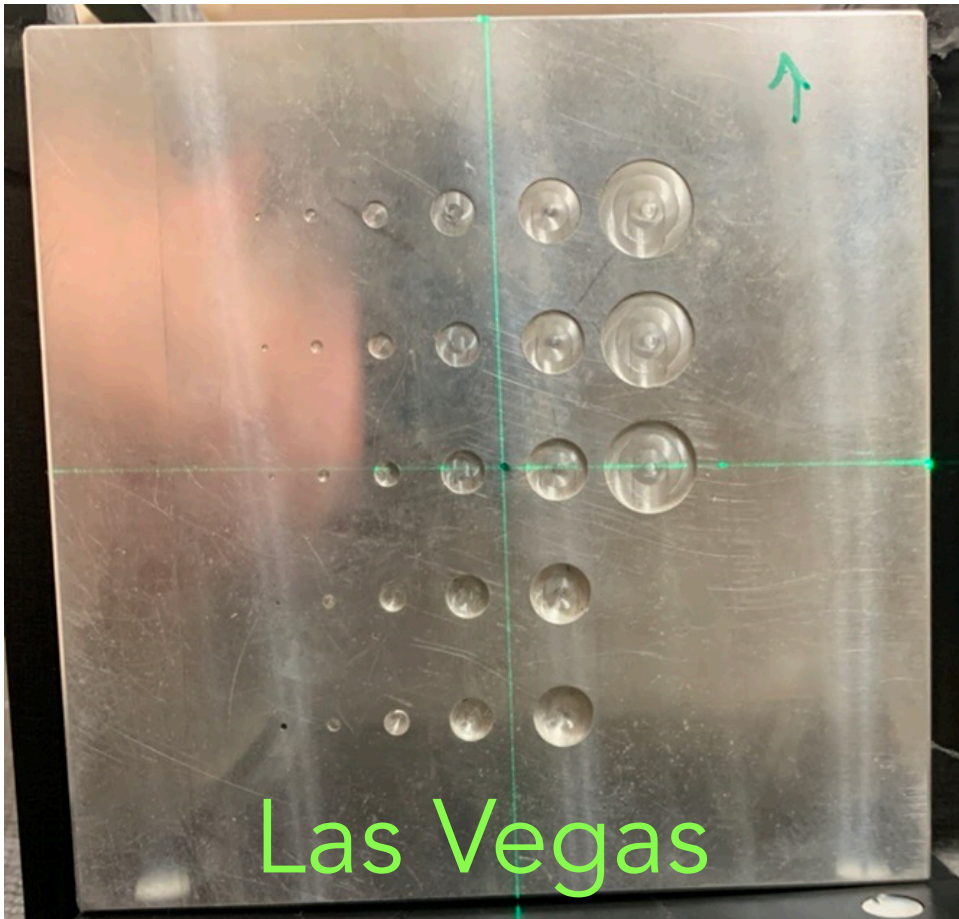
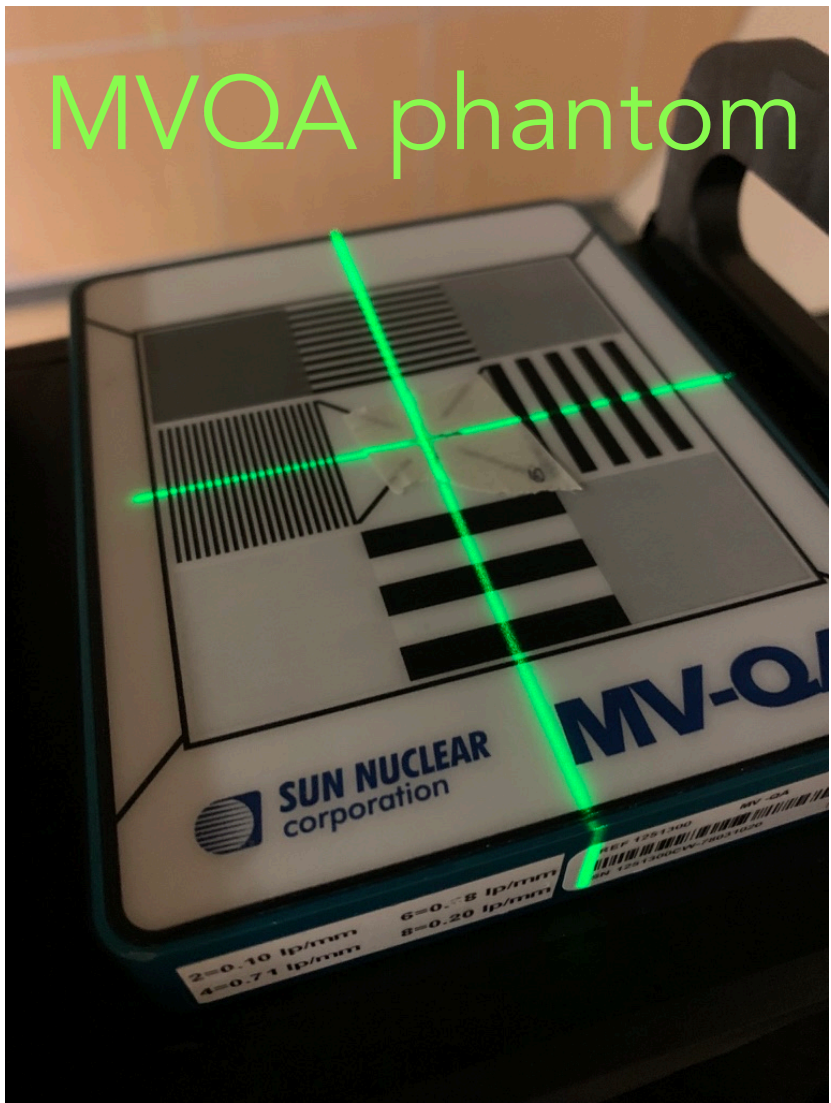
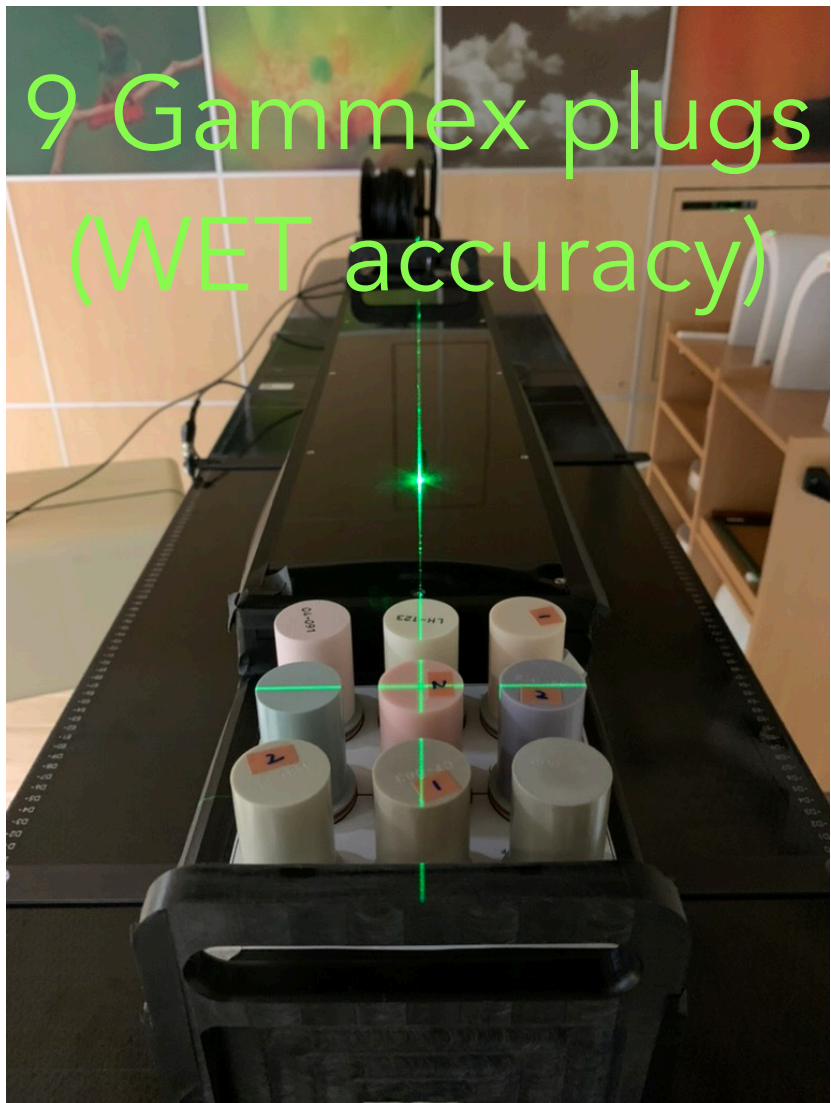
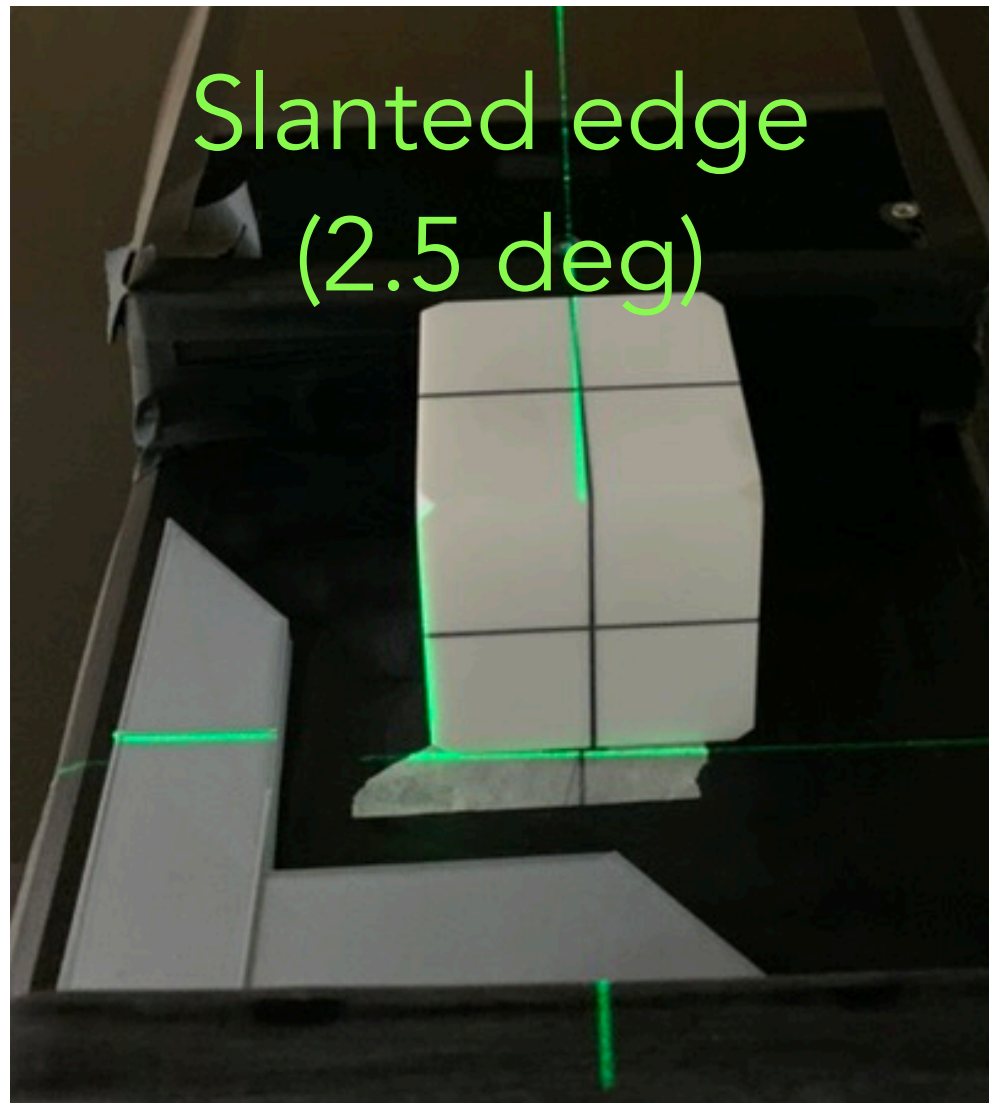
Beam parameters

| | |
|--------------------|--|
| Energy | 200 MeV |
| Spot size | 3 mm |
| Angular divergence | 3 mrad |
| Beam spacings | 1 mm (allows to sample other spacings) |

Example of 10 mm spacing sampling



Methods - phantoms & imaging parameters



- The **scintillator** is a 10x10x10 cm cube, allowing a **10x10 cm² FOV**.
- Slanted edge, Gammex, MVQA & Las Vegas:
- Paediatric phantom:

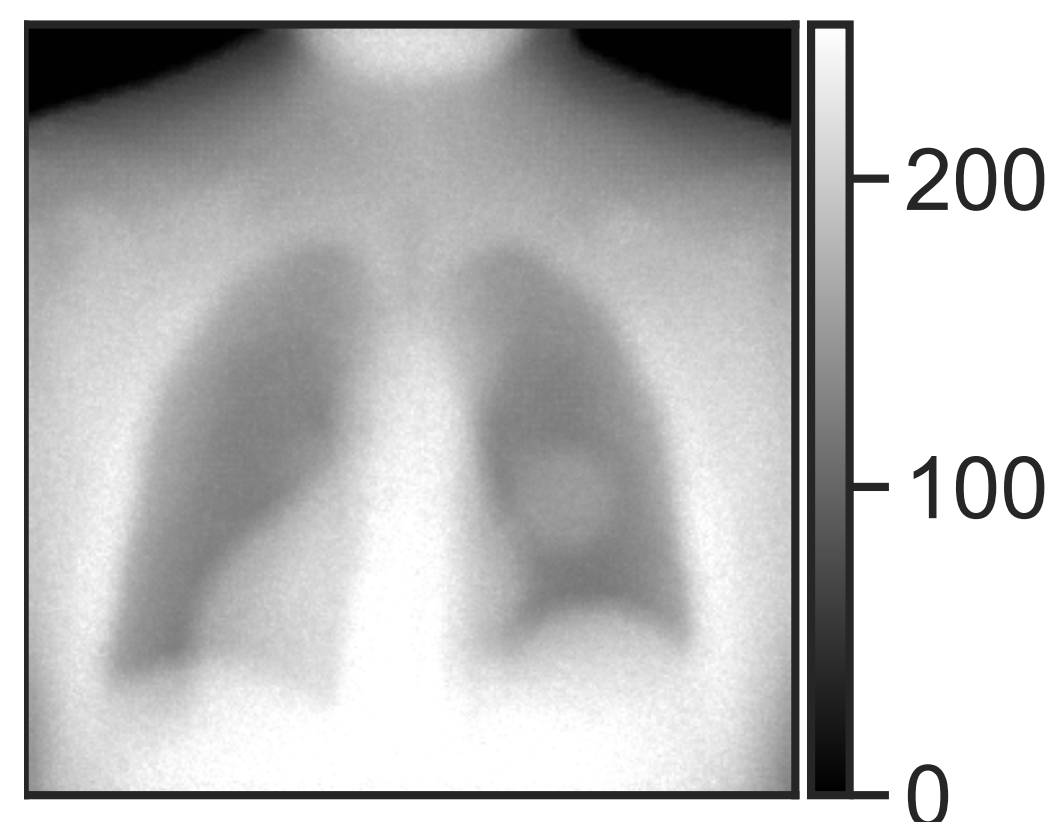
| | |
|---------------|------------------|
| Camera FOV | 10x10 cm |
| Energy | 135.6 MeV |
| Spot size | 3.1 mm |
| Beam spacings | 2, 3, 4 and 5 mm |

| | |
|---------------|------------------|
| Camera FOV | 10x10 cm |
| Energy | 189 MeV |
| Spot size | 2.5 mm |
| Beam spacings | 2, 3, 4 and 5 mm |

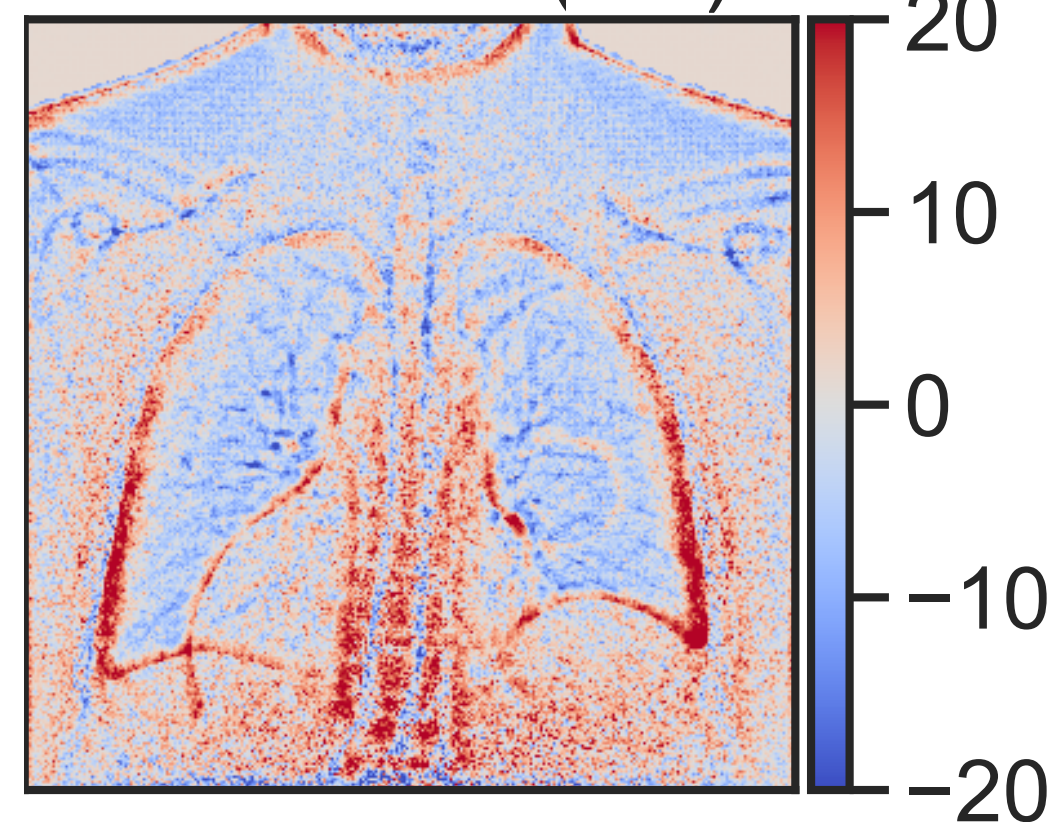
Image corrections: see R. Fullarton's talk Friday for details.

MC Results - XCAT (200 MeV) - comparing recons

2D distal view

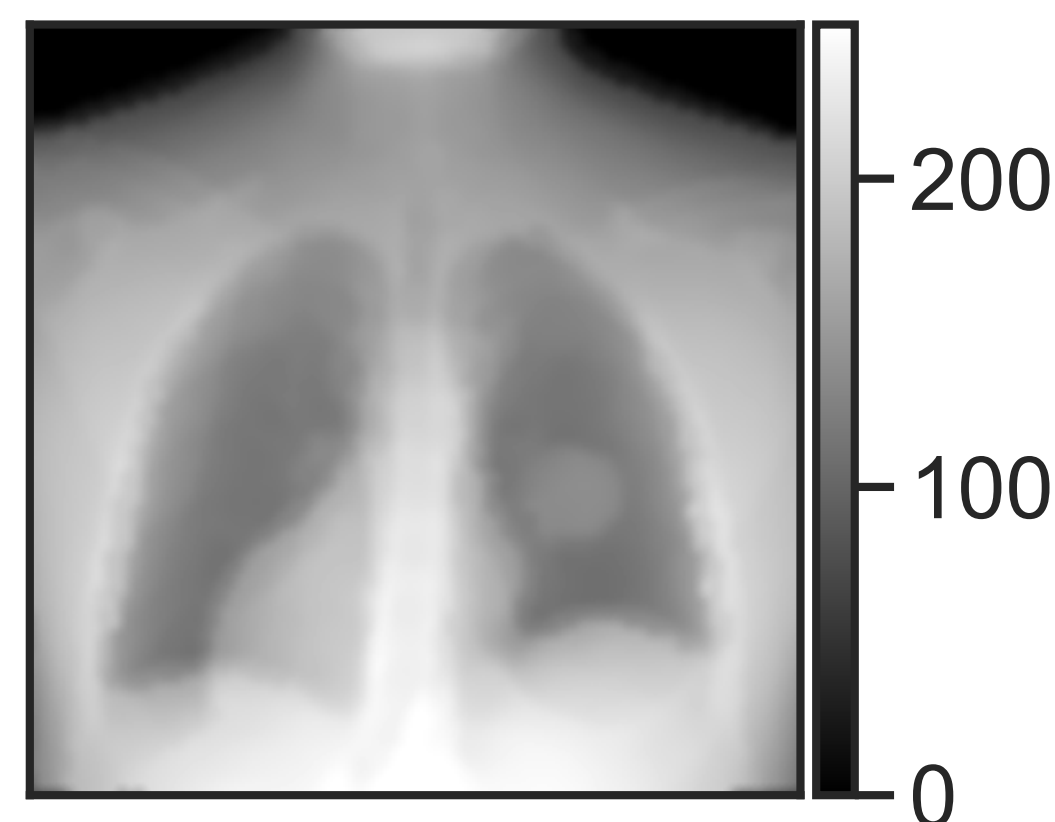


WET error (mm)

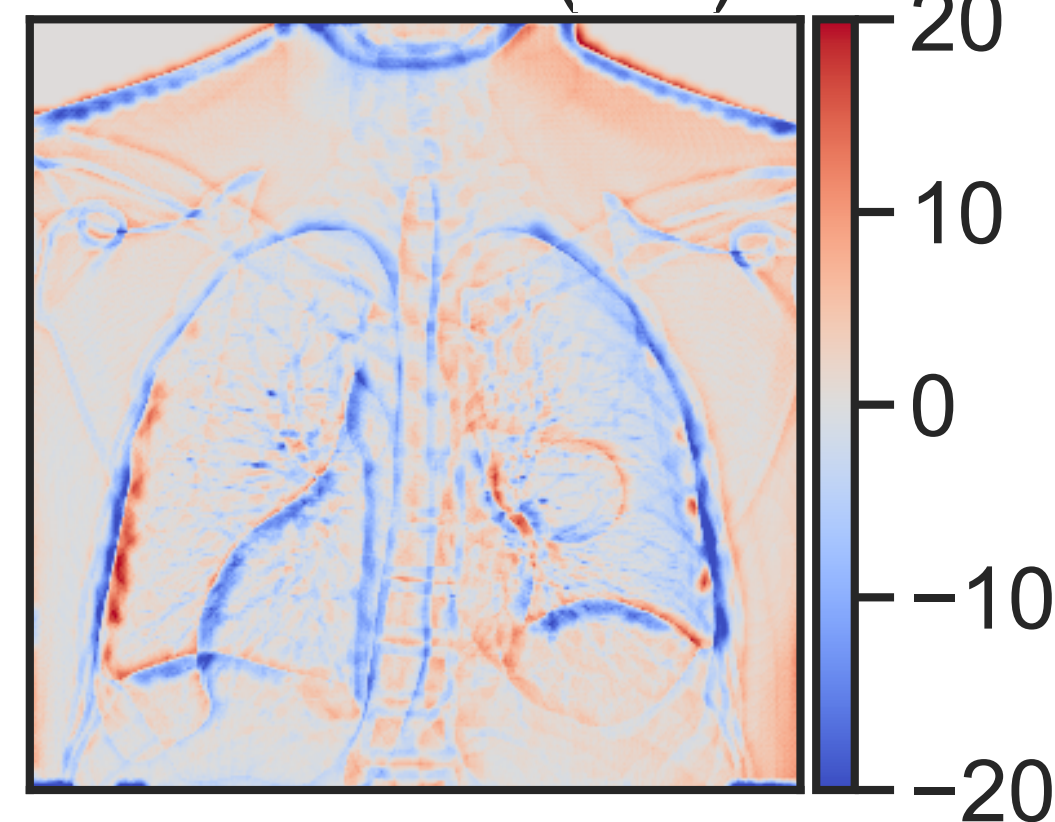


5.8 mm

1D lateral view

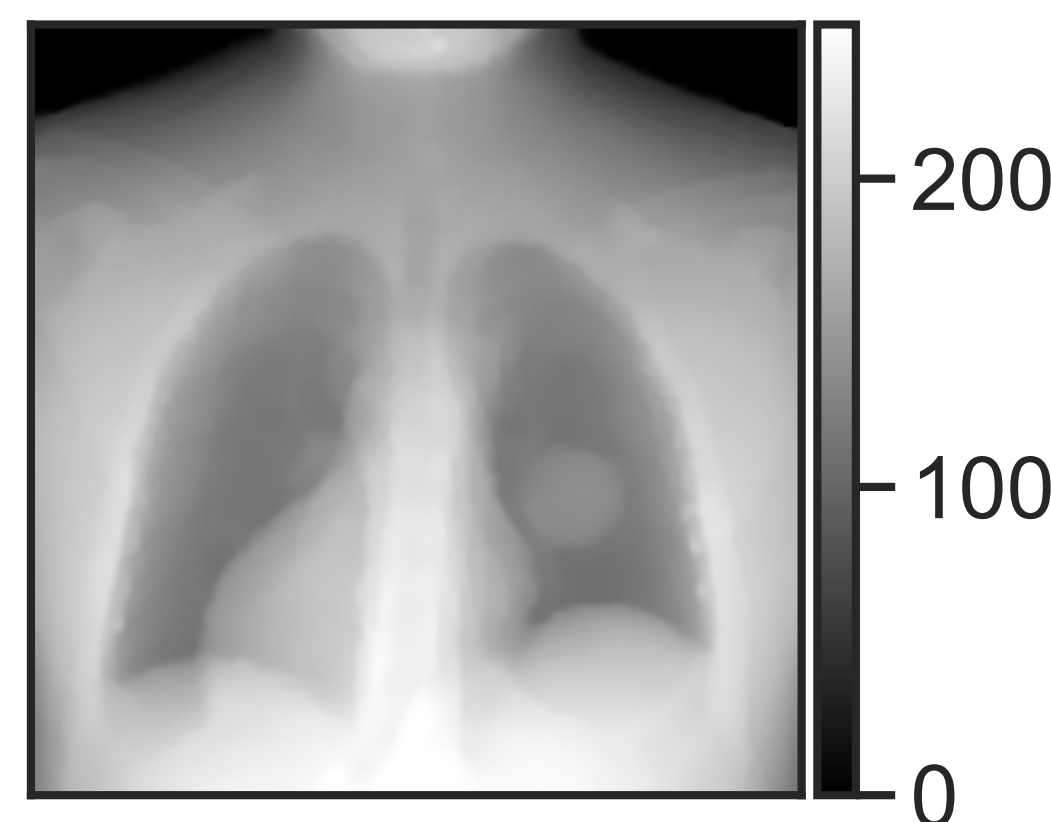


WET error (mm)

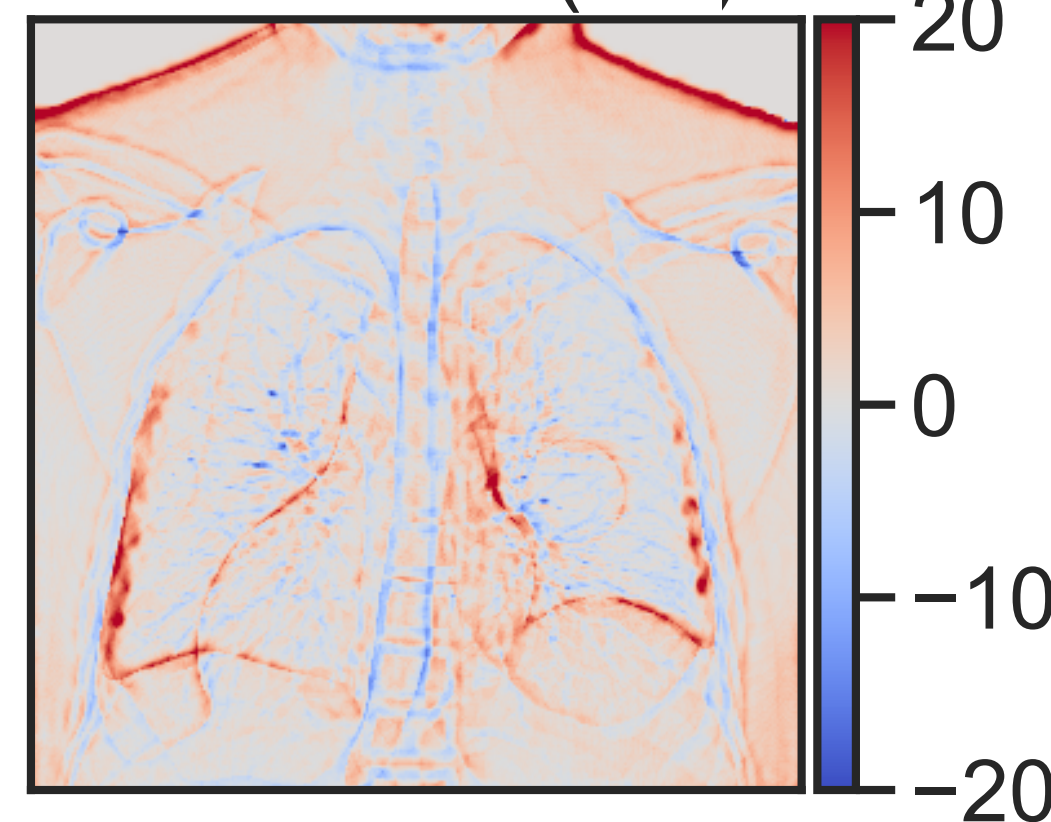


3.2 mm

2x2D lateral views

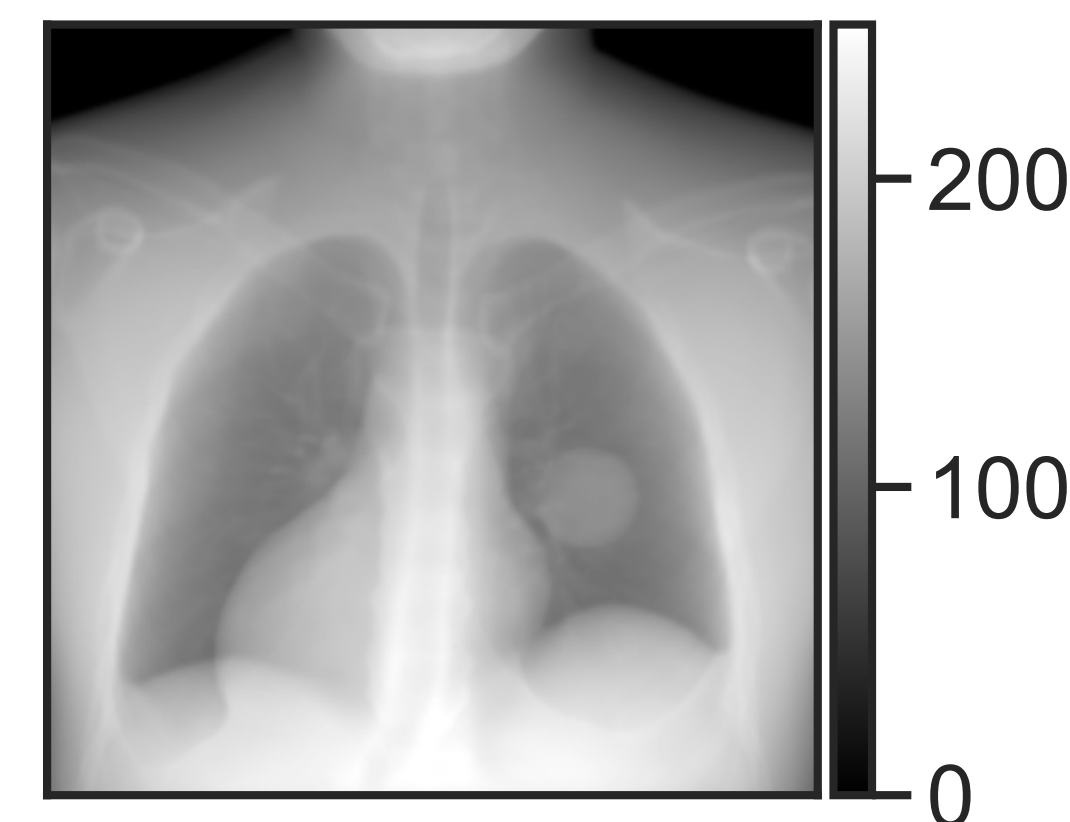


WET error (mm)

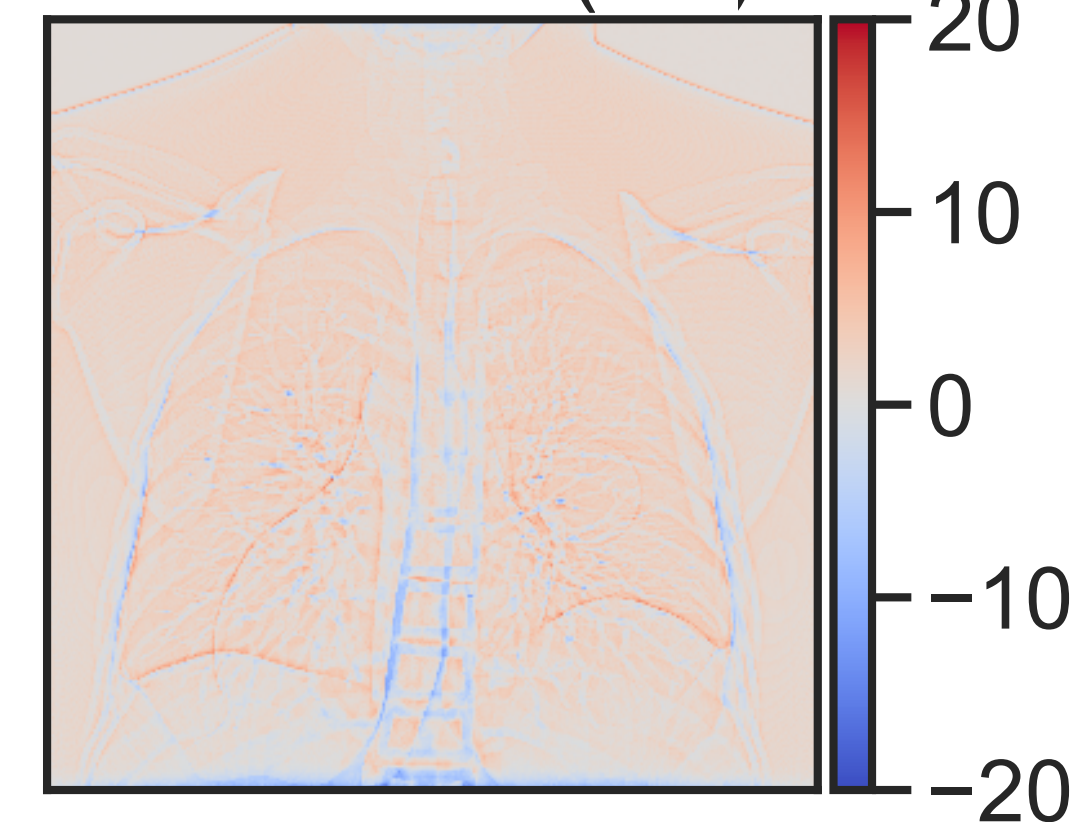


2.6 mm

Single event imaging



WET error (mm)



2.1 mm

MAE

- Integrated mode images (distal, lateral 1D and 2D) use a 3 mm sampling (5625 PBs).

MC Results - XCAT (200 MeV) - impact of spacing

- Reconstruction method: 2x2D lateral views.

- Reminder: **large FOV** of 30x30 cm².

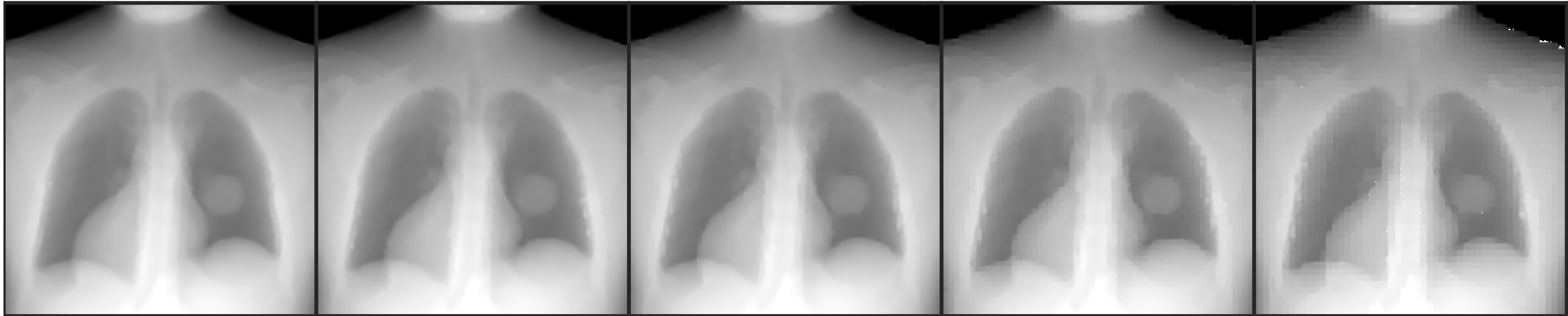
2 mm

3 mm

4 mm

5 mm

6 mm



22801 PBs

10201 PBs

5625 PBs

3600 PBs

2500 PBs

MC Results - XCAT (200 MeV) - impact of spacing

* Assuming 3 ms / PB (low dose).

- **Reconstruction method:** 2x2D lateral views.

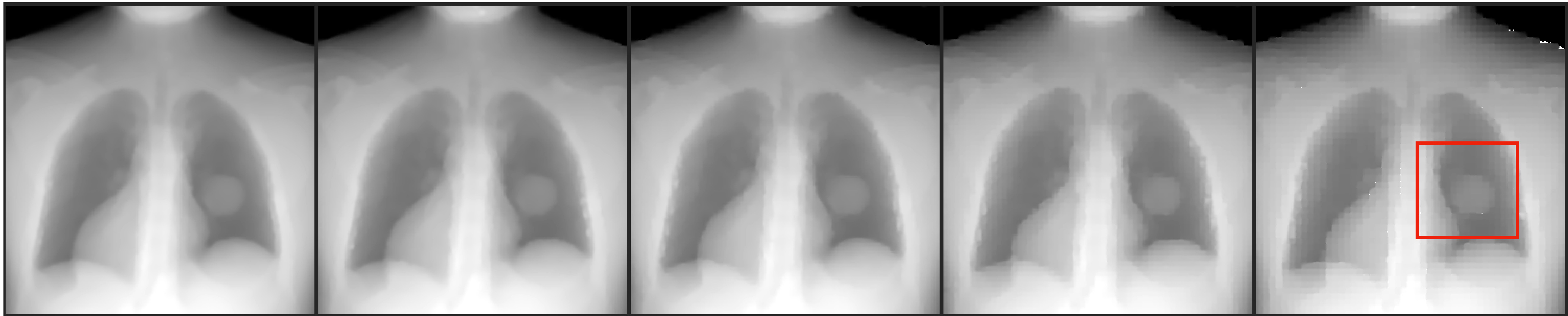
2 mm

3 mm

4 mm

5 mm

6 mm



22801 PBs

10201 PBs

5625 PBs

3600 PBs

2500 PBs

(68 s)*

(30 s)*

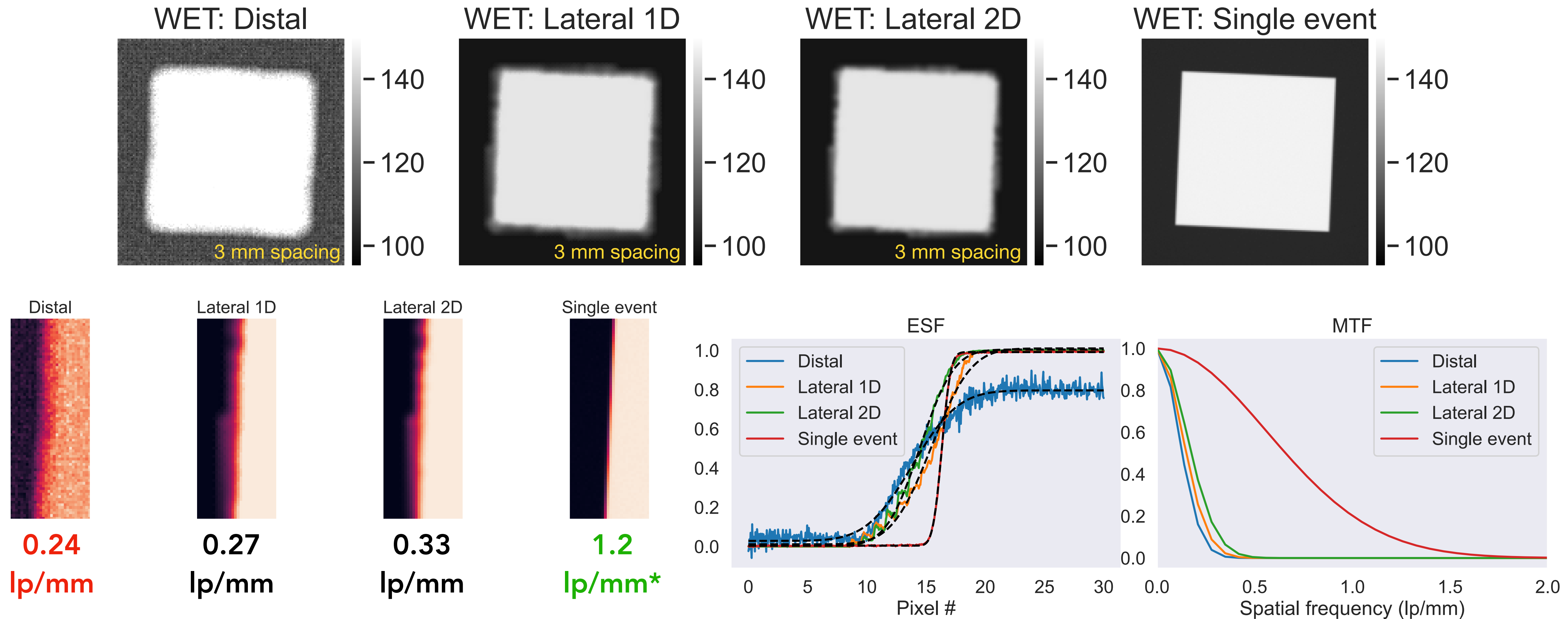
(17 s)*

(11 s)*

(7.5 s)*

- Possibility of creating large FOV images in <10s with acceptable image quality.
- Reducing the FOV to 10x10 cm² with 6 mm spacing could reduce imaging time to <1s.

MC Results - slanted edge (200 MeV)



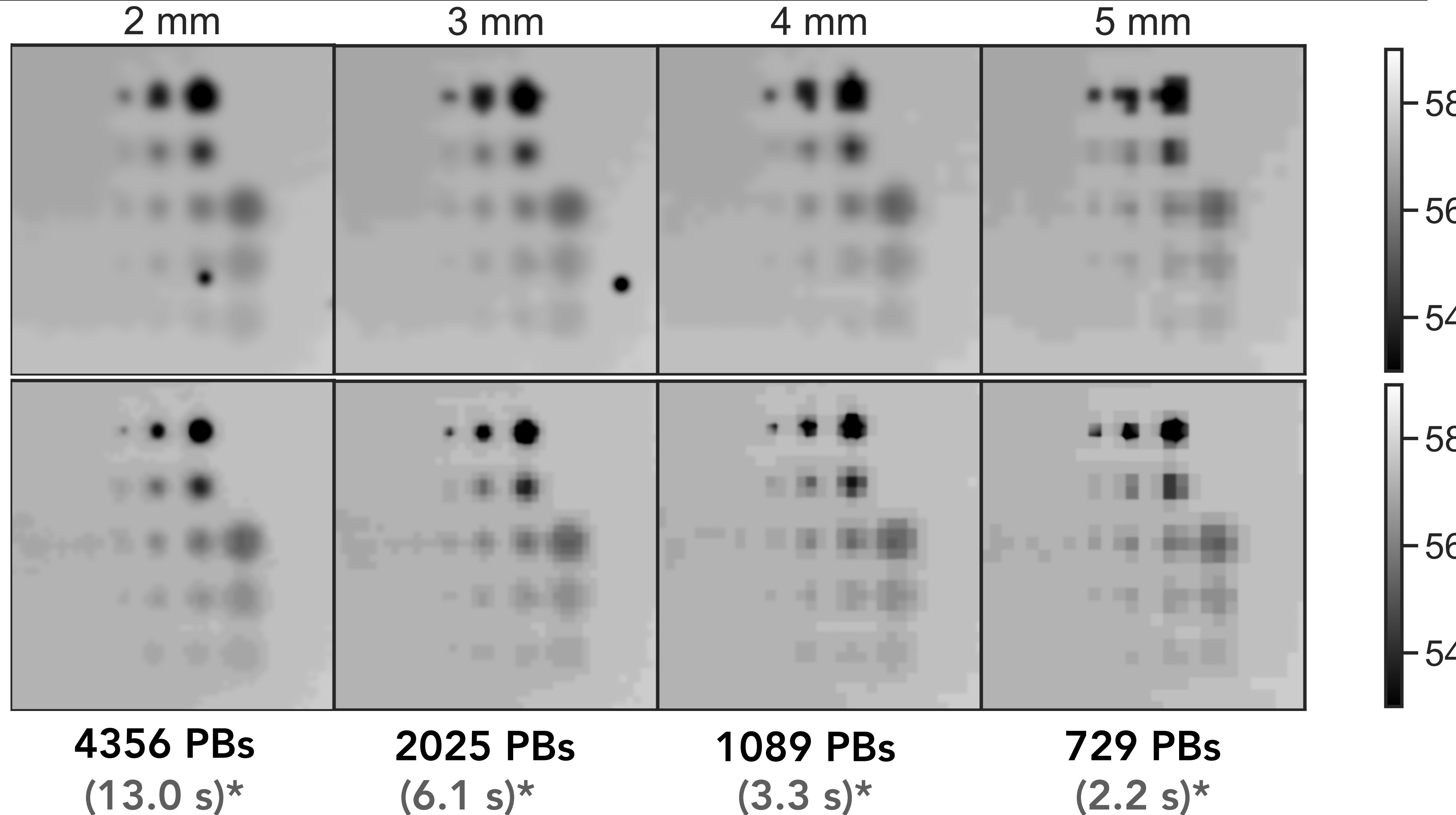
*Matches literature values [7,8] for ideal trackers - realistic trackers would provide a fairer comparison.

Exp. results - Las Vegas (135 MeV) - impact of spacing & recon

- The LV phantom contains very small objects to resolve (FOV is 10x10 cm²). The impact of PB spacing is clear, with small objects becoming distorted with large spacing.
- Images with the 2D method appear less blurry than 1D.

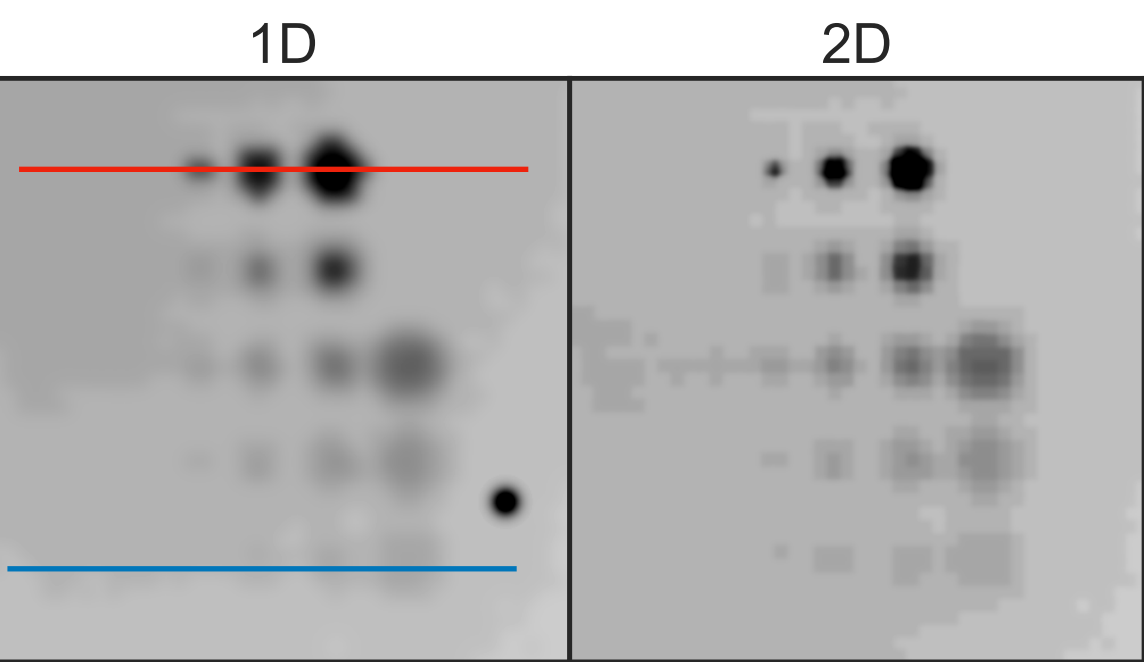
1D
lateral
view

2x2D
lateral
views



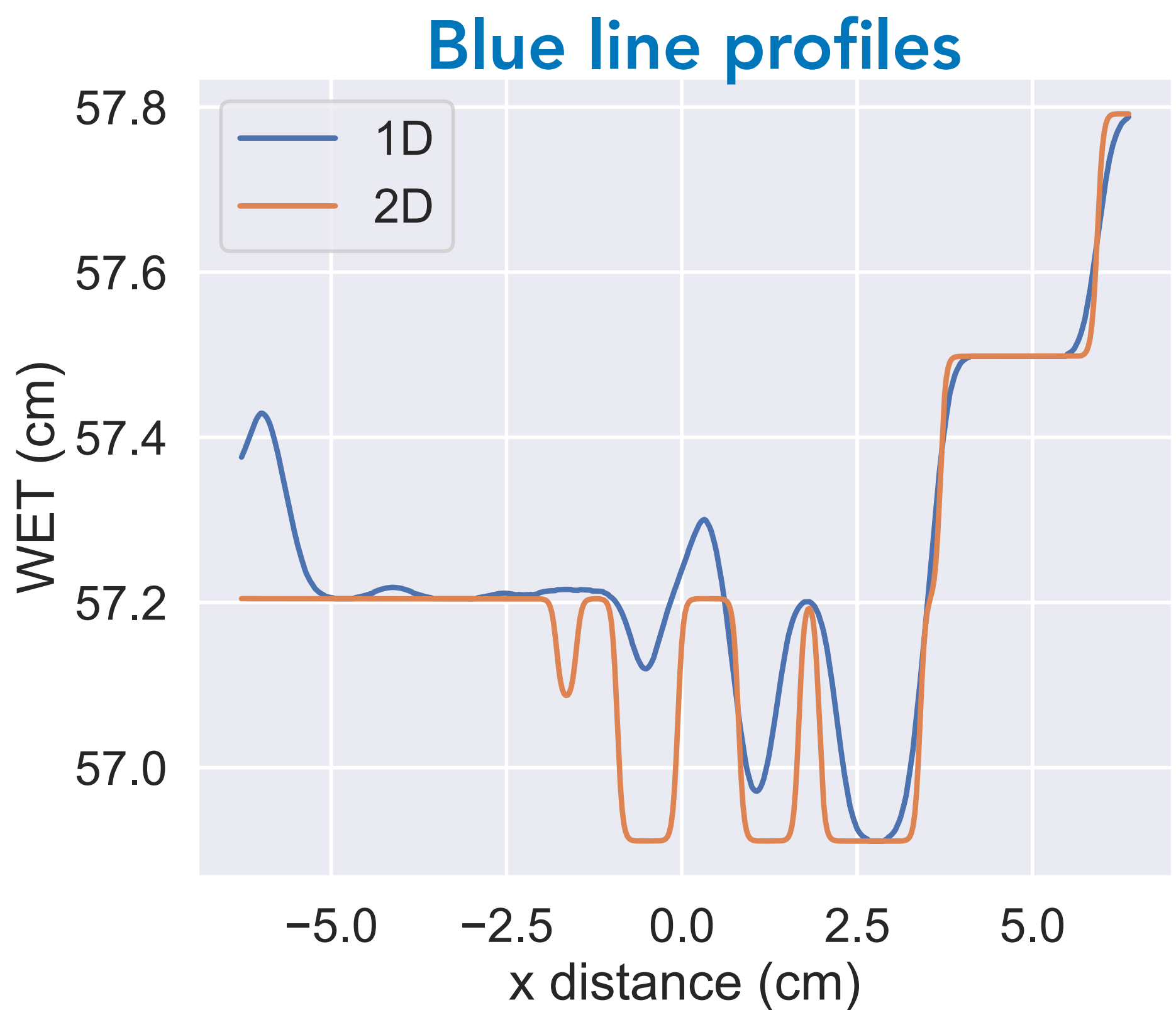
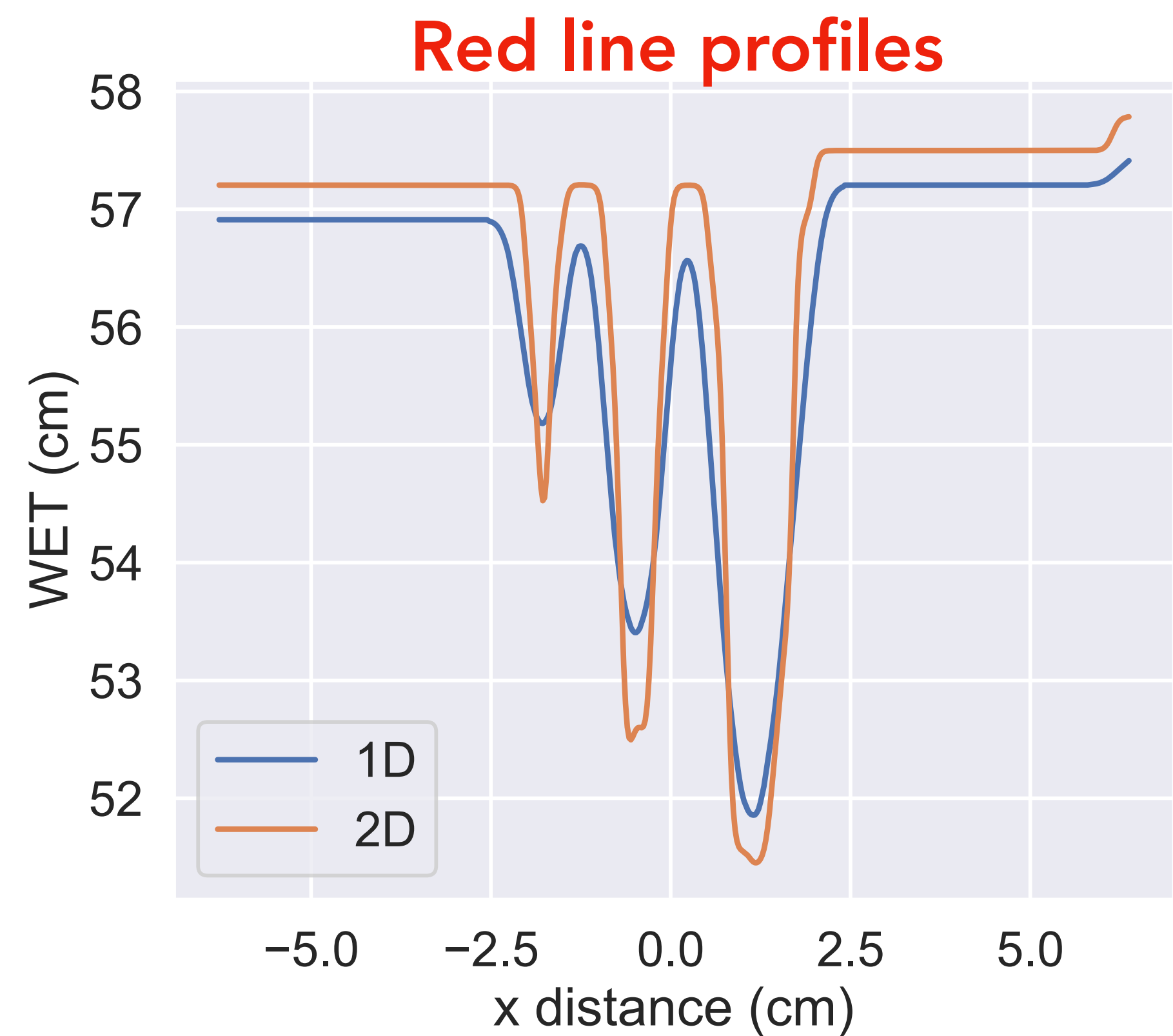
Exp. results - Las Vegas (135 MeV) - impact of recon

- Clear increase in **contrast** with the 2D approach compared to the 1D method.



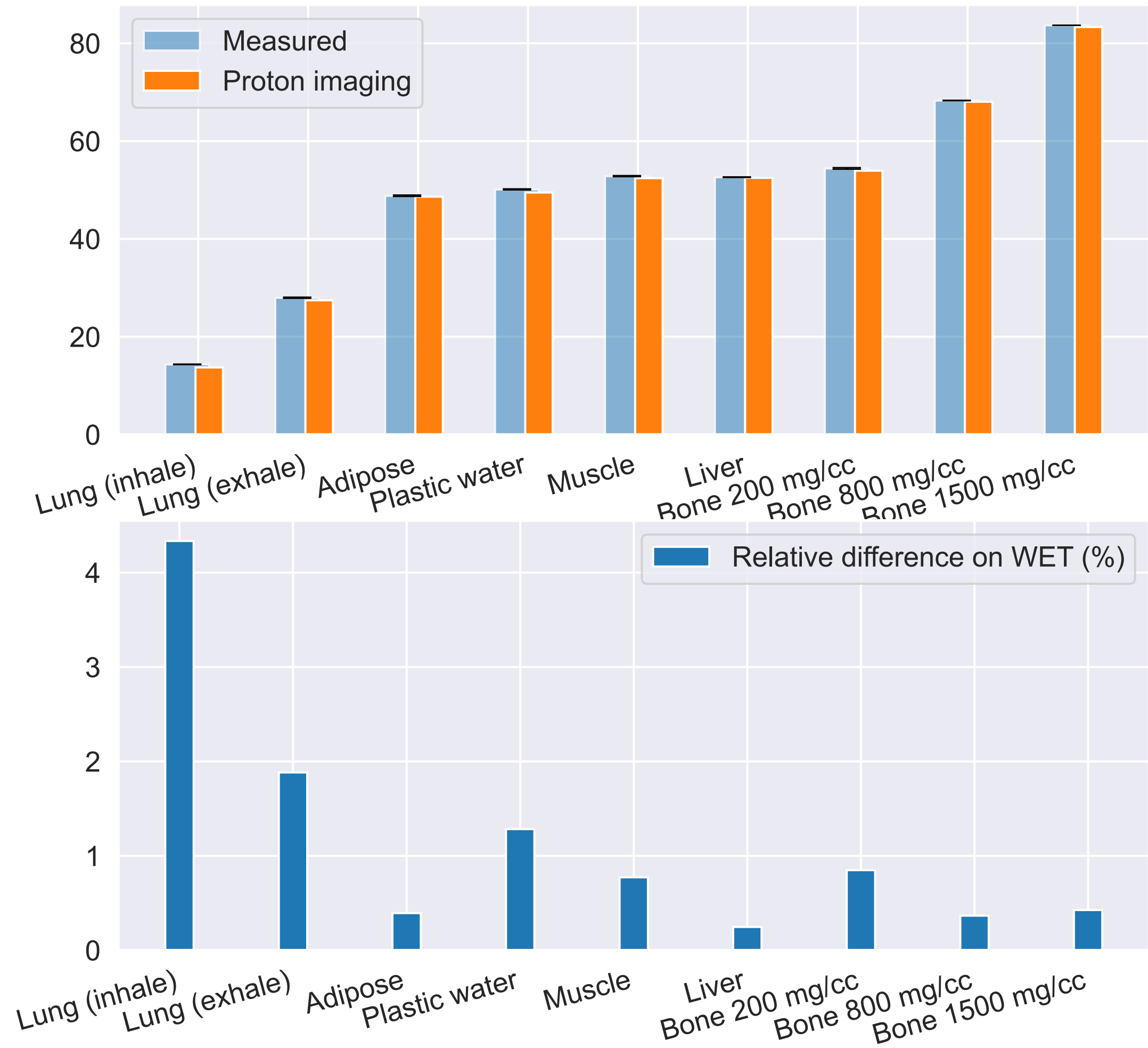
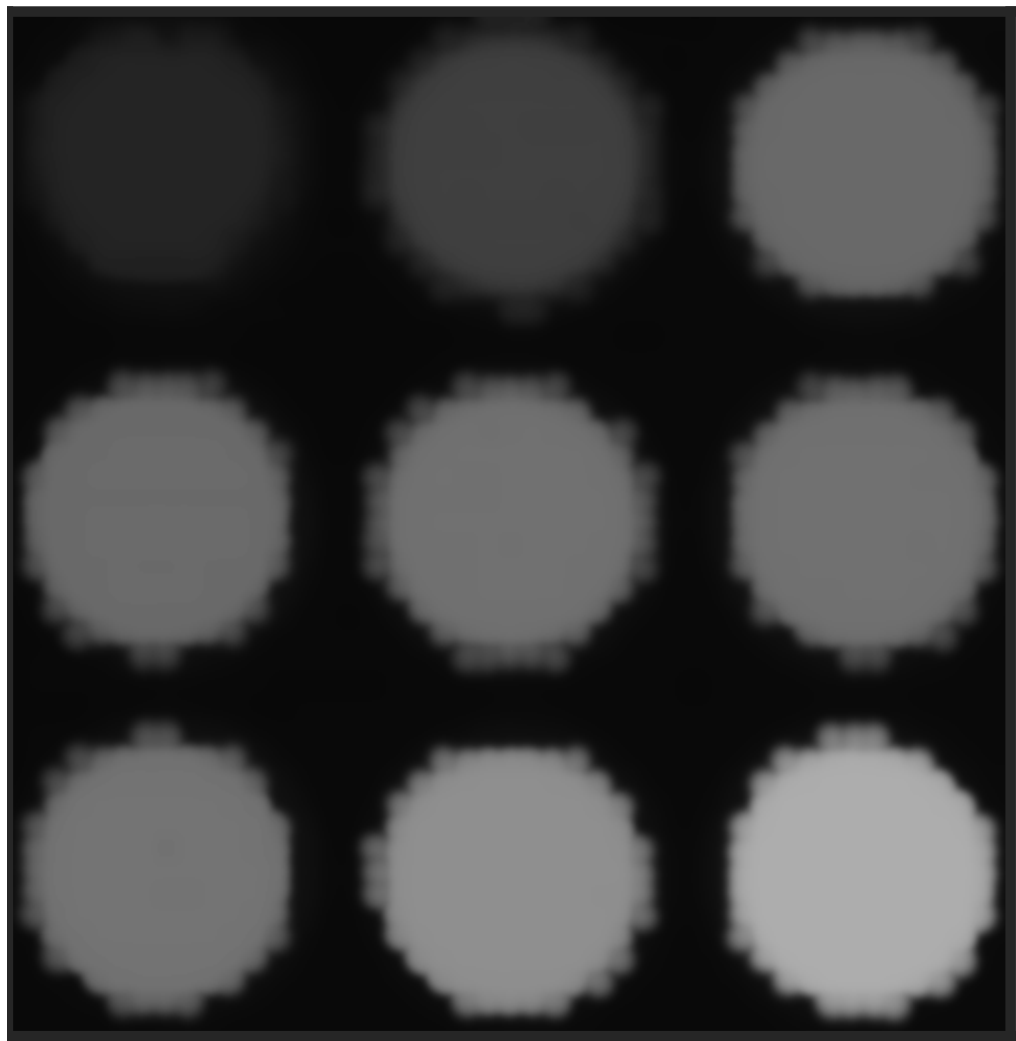
| | | Hole Diameter (mm) | | | | | | % Contrast | |
|-----------------|------|--------------------|---|---|---|----|----|------------|-----|
| | | 0.5 | 2 | 4 | 7 | 10 | 15 | | |
| Hole Depth (mm) | 4.5 | • | • | • | • | • | • | 5.1 | 3.4 |
| | 3.25 | • | • | • | • | • | • | 3.7 | 2.5 |
| | 2.0 | • | • | • | • | • | • | 2.3 | 1.5 |
| | 1.0 | • | • | • | • | • | • | 1.2 | 0.8 |
| | 0.5 | • | • | • | • | • | • | 0.6 | 0.4 |

6MV 15MV



Exp. results - WET accuracy (135 MeV, 3 mm spacing)

- Reconstruction method: 2x2D lateral views.



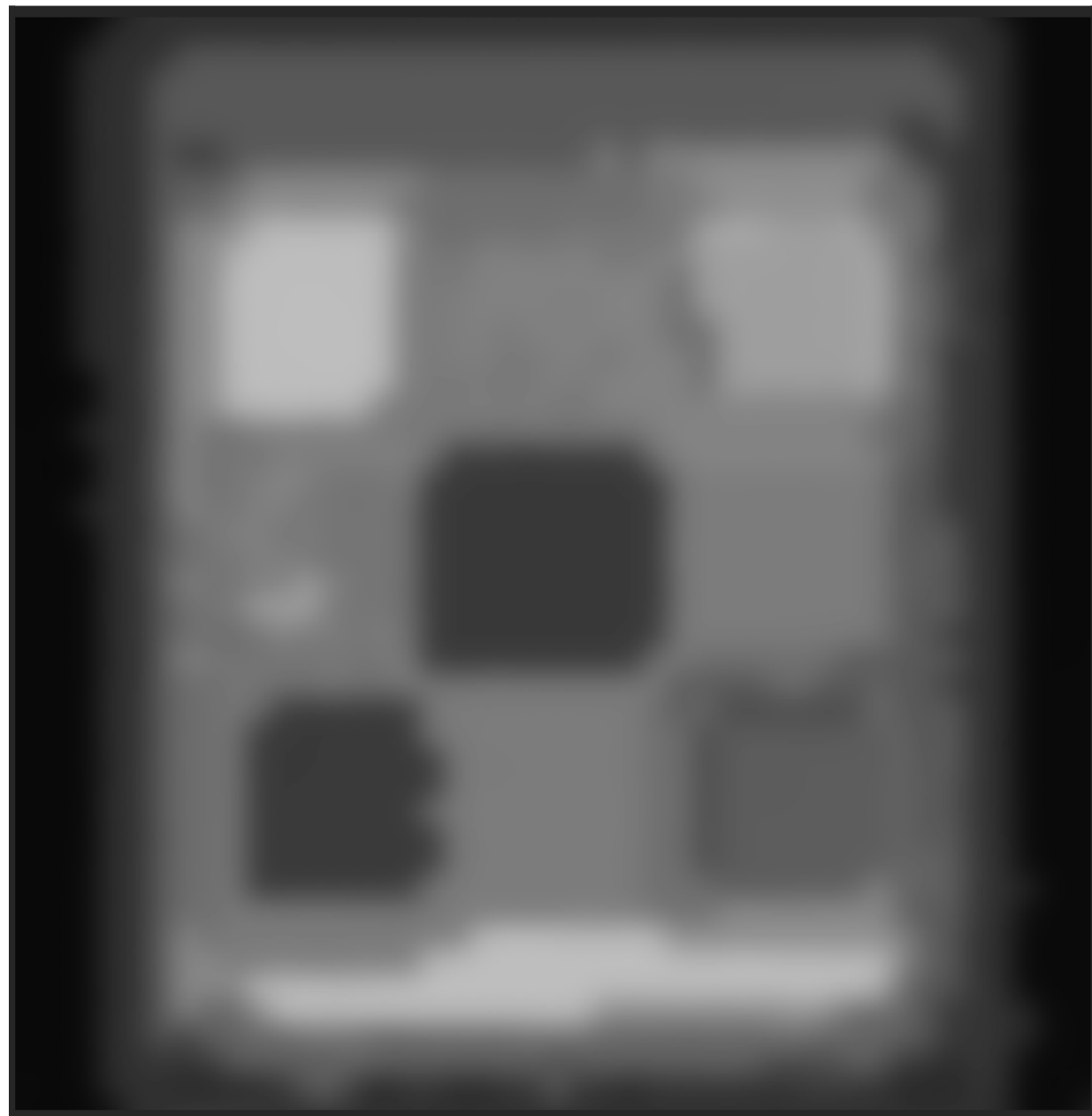
Mean absolute error (MAE) over all plugs

Relative: 1.2%
Absolute: 0.4 mm

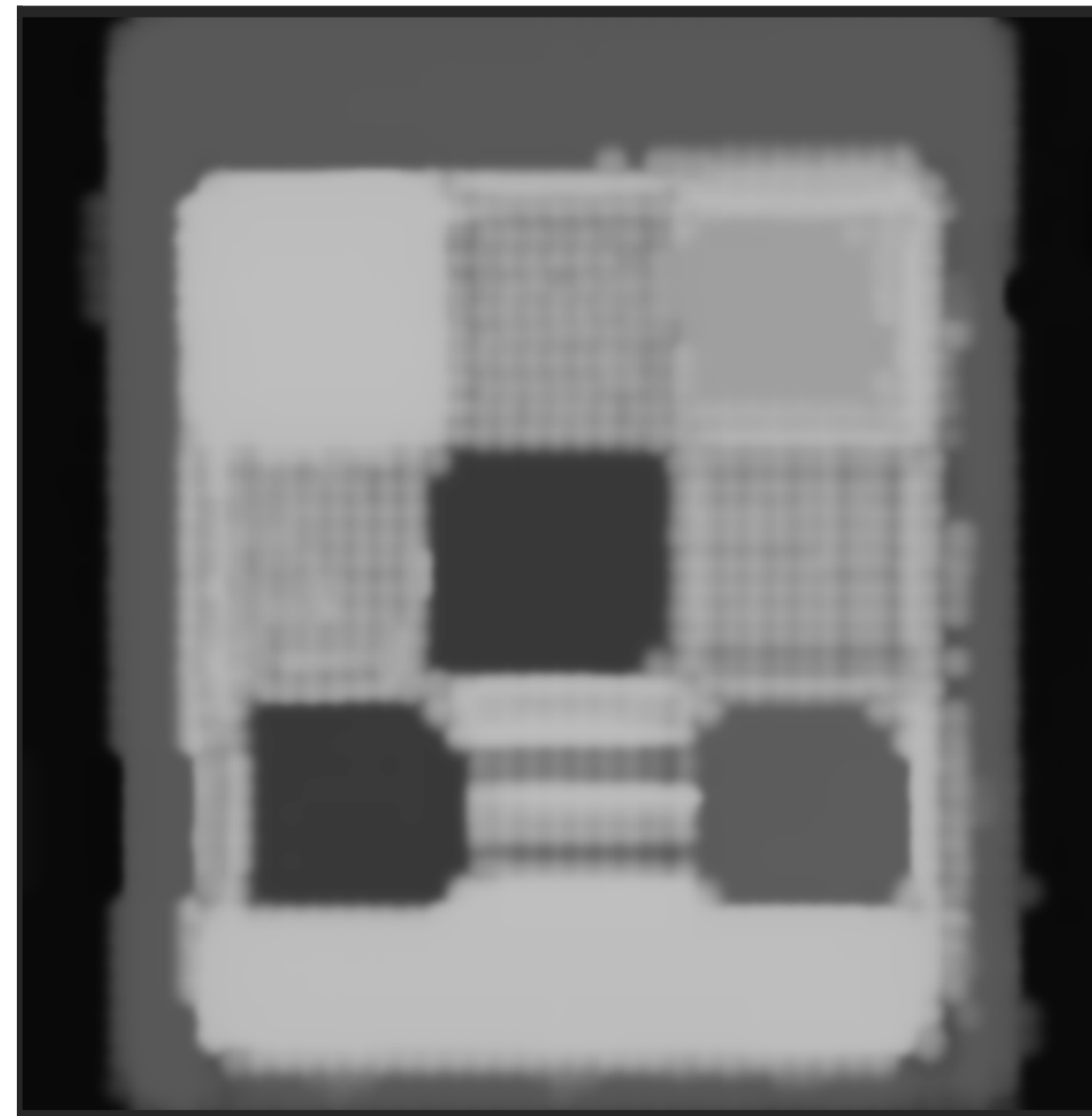
Exp. results - MVQA phantom (135 MeV, 3 mm spacing)

- Misalignment issues between lateral views acquisition increases blur, may have degraded 2D.
- **Very complex scintillation images to analyse (multiple BPs) -> reduced performance of 1D.**
- 2D: 0.1 lp/mm module visible, 0.2 lp/mm can almost be resolved on right hand side (see third image).

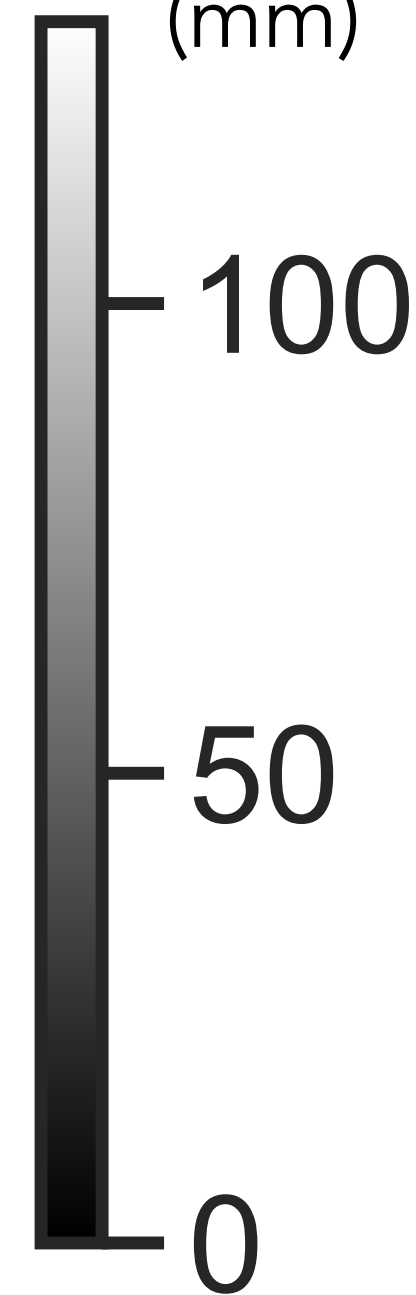
1D lateral view



2x2D lateral views

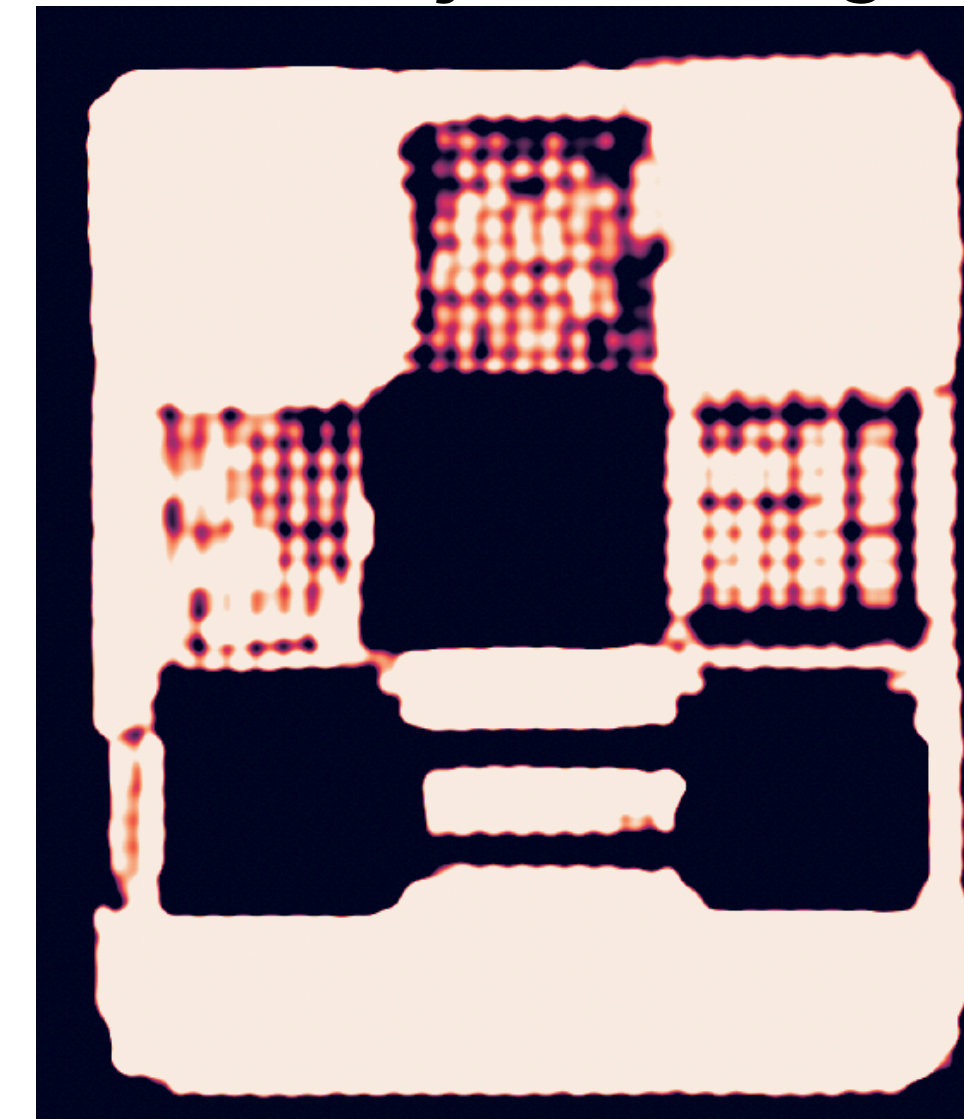


WET
(mm)



2D

(smaller dynamic range)

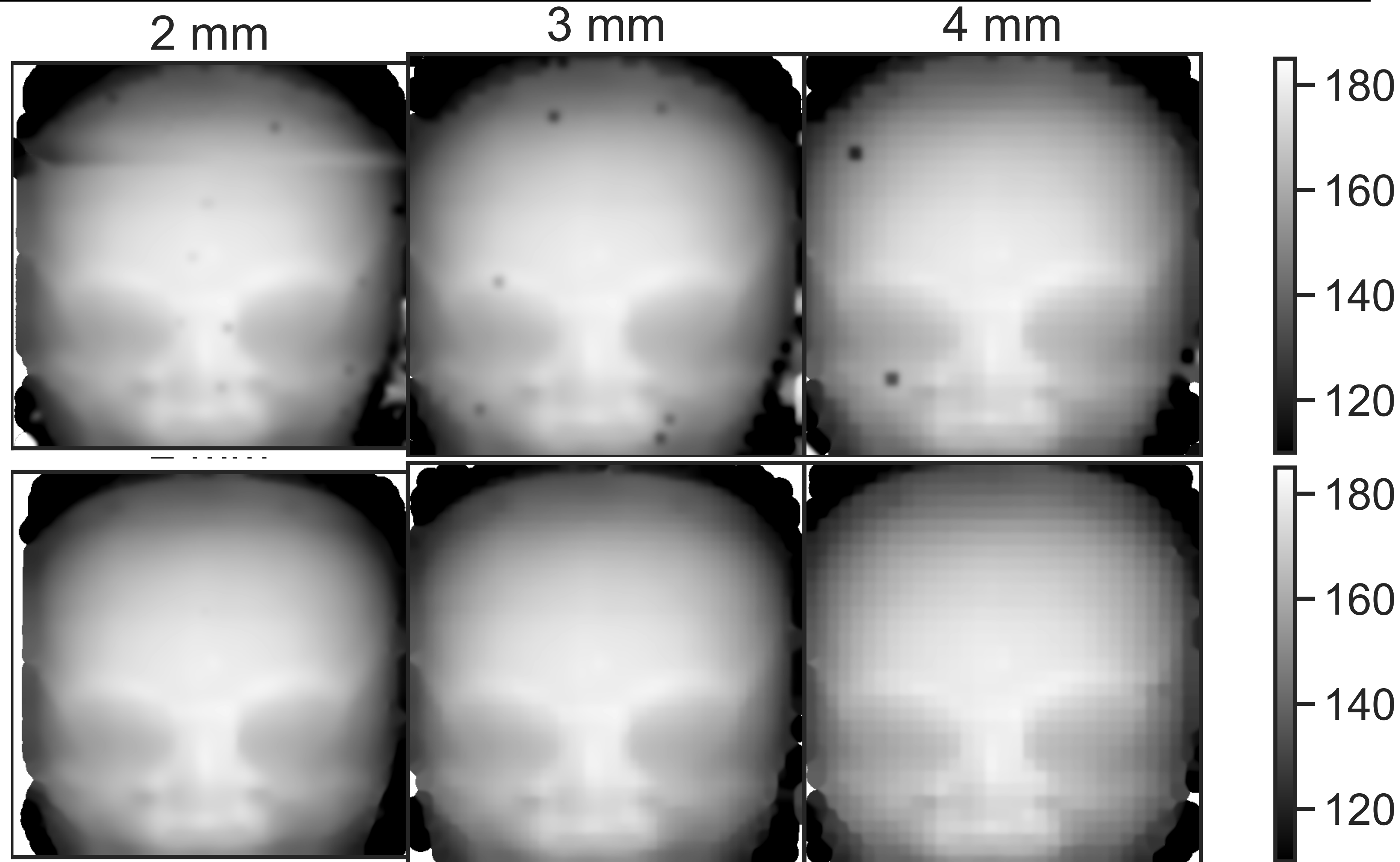


Exp. results - Paediatric head phantom (189 MeV) - impact of spacing

- **Increased blur** with respect to previous phantoms due to phantom size (more scatter).
- Possibly need to improve **data processing** (camera PSF, peakfinder issues) to obtain clear benefits of 2D.

1D
lateral
view

2x2D
lateral
views

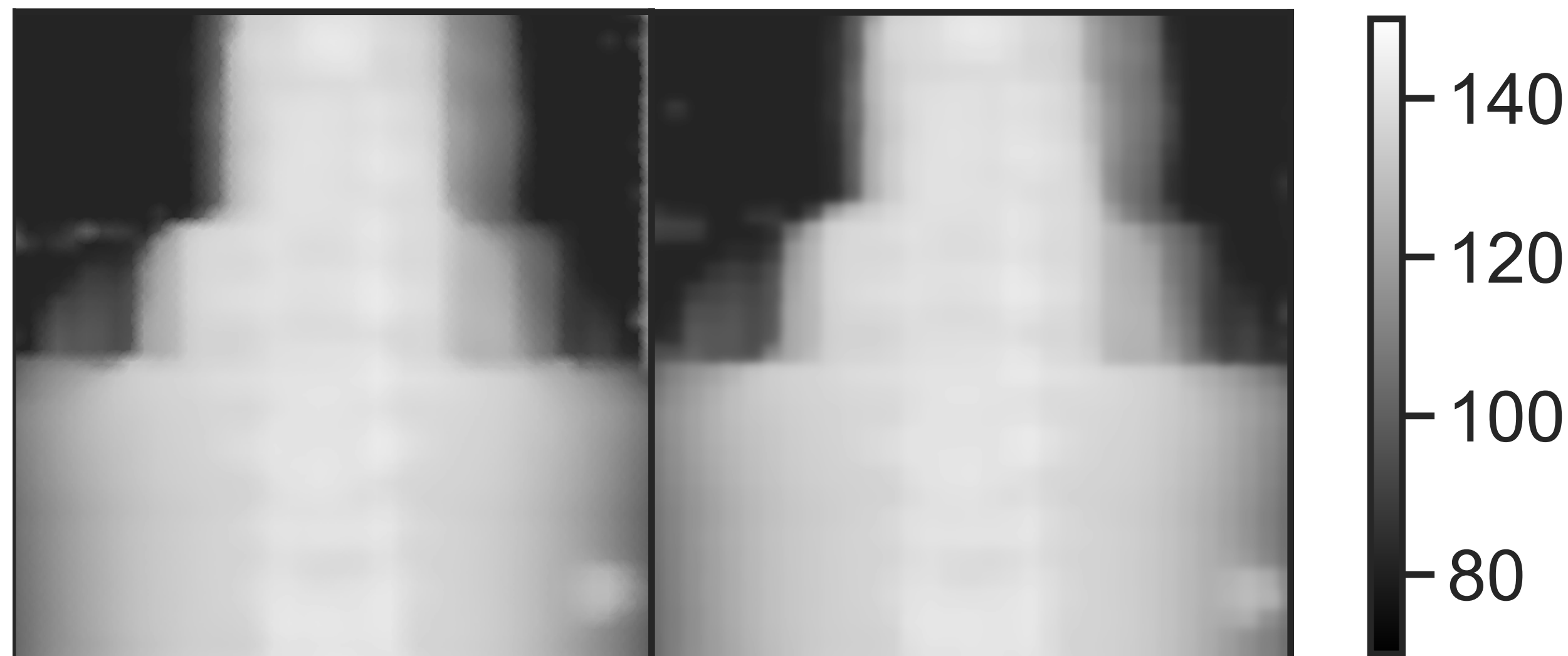


Exp. results - Paediatric thorax phantom (189 MeV) - impact of spacing

- Reconstruction shown: **2x2D lateral views reconstruction**.
- Two dynamic ranges to highlight different structures.
- ROI is not well centred on structures of interest, but allows to clearly see the soft tissue/lung interface.

3 mm

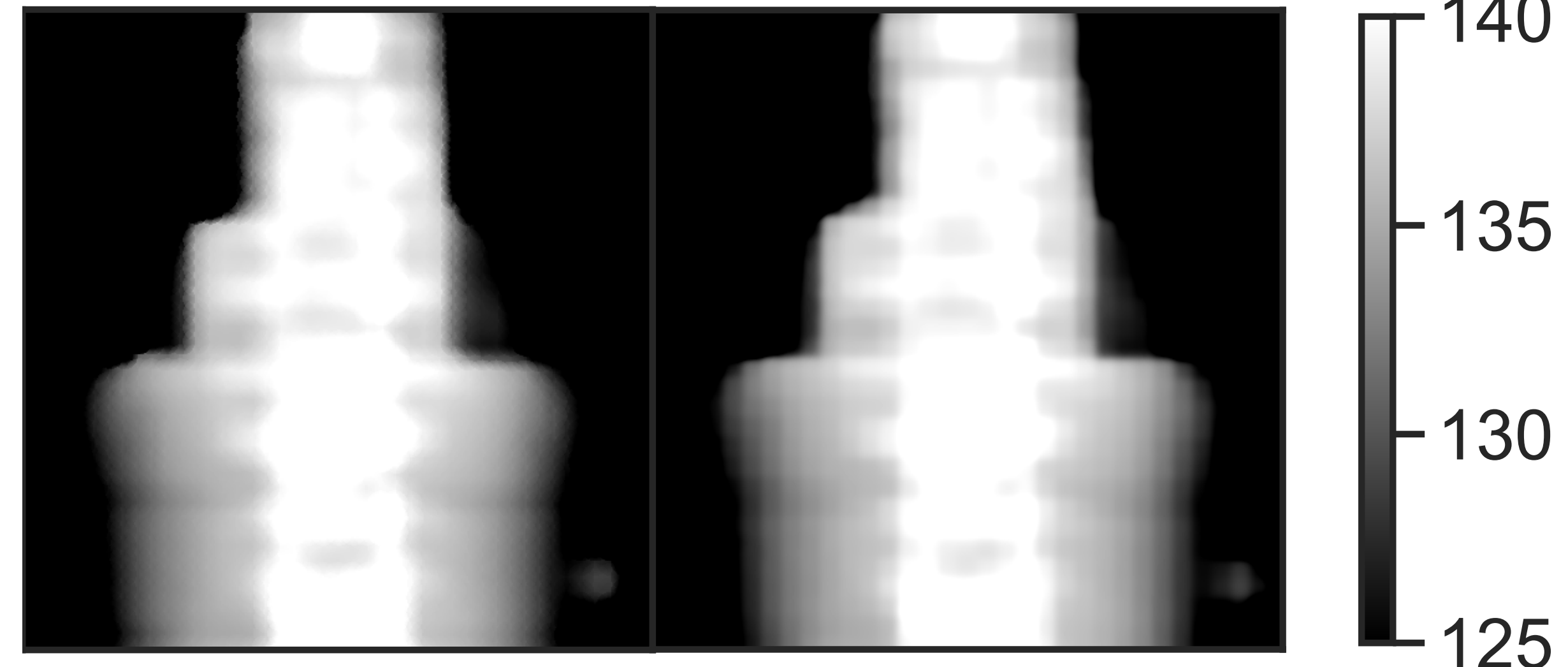
4 mm



highlight all structures

3 mm

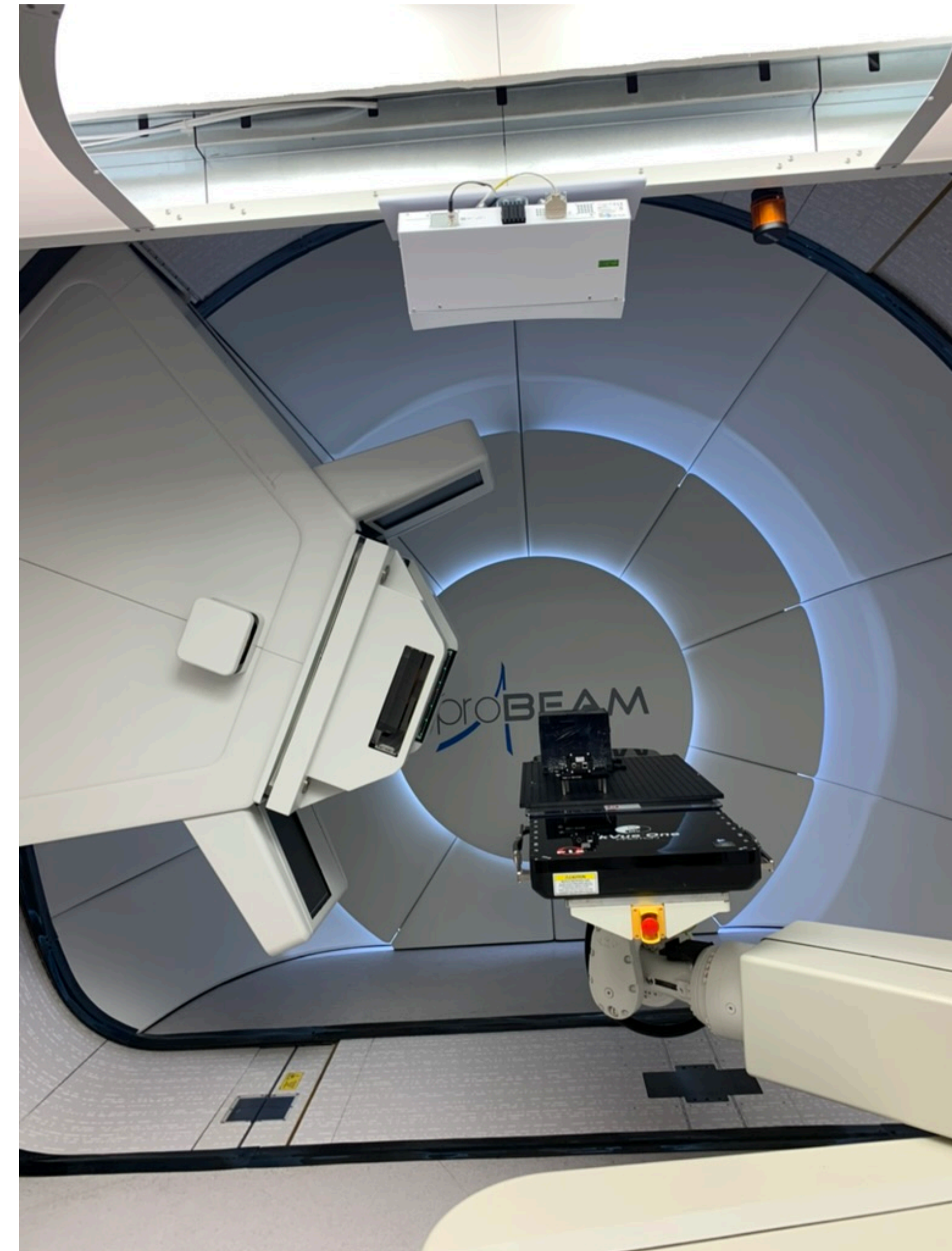
4 mm



highlight spine

Conclusions

- Using **2D signals with the 2 lateral views** combined with the **proposed algorithm** provides **improved image quality** with respect to **published integrated mode imaging approaches** (1D signal or 2D signal with distal view).
- Results suggest that pRads can be acquired **rapidly** (<1 s), using a system that is **low cost** (<£10k) and **easily integrable** (all images taken with clinical settings).
- Next steps are to maximise image quality with experimental data:
 - deconvolve camera PSF
 - correct for camera spatial distortions
 - improve the performance of the peakfinder or infer $\frac{N_i(\mathbf{r}_d)}{N_{i,\text{tot}}}$.



Acknowledgements

- This project has received funding from the European Union's Horizon 2020 research and innovation programme under the Marie Skłodowska-Curie grant agreement No 101023220.
- UCL Global engagement fund
- UCL Devices & Diagnostics TIN Pilot Data Scheme
- Lennart Voltz from insightful discussions



Horizon 2020
European Union funding
for Research & Innovation

Extra slides

Methods - experimental setup (Mayo Clinic Arizona)

- The **scintillator** is a 10x10x10 cm cube, allowing a **10x10 cm² FOV**.
- **Two lateral views** are acquired by moving the couch.



- To fix the object position for the two lateral views and reduce positioning errors, the following setup is adopted.

phantom goes here

additional couch
serving as
phantom holder

Water tank with
adjustable height/tilt

